Gauge-independent off-shell fermion self-energies at two loops: The cases of QED and QCD

Daniele Binosi* and Joannis Papavassiliou†
Departamento de Física Teórica and IFIC, Centro Mixto, Universidad de Valencia-CSIC, E-46100, Burjassot, Valencia, Spain
(Received 17 October 2001; published 19 March 2002)

We use the pinch technique formalism to construct the gauge-independent off-shell two-loop fermion self-energy, both for Abelian (QED) and non-Abelian (QCD) gauge theories. The new key observation is that all contributions originating from the longitudinal parts of gauge boson propagators, by virtue of the elementary tree-level Ward identities they trigger, give rise to effective vertices, which do not exist in the original Lagrangian; all such vertices cancel diagrammatically inside physical quantities, such as current correlation functions or *S*-matrix elements. We present two different, but complementary derivations: First, we explicitly track down the aforementioned cancellations inside two-loop diagrams, resorting to nothing more than basic algebraic manipulations. Second, we present an absorptive derivation, exploiting the unitarity of the *S* matrix, and the Ward identities imposed at the tree level and one-loop physical amplitudes by gauge invariance, in the case of QED, or by the underlying Becchi-Rouet-Stora symmetry, in the case of QCD. The propagatorlike subamplitude defined by means of this latter construction corresponds precisely to the imaginary parts of the effective self-energy obtained in the former case; the real part may be obtained from a (twice subtracted) dispersion relation. As in the one-loop case, the final two-loop fermion self-energy constructed using either method coincides with the conventional fermion self-energy computed in the Feynman gauge.

DOI: 10.1103/PhysRevD.65.085003 PACS number(s): 11.15.Bt, 12.38.Bx, 14.60.−z, 14.65.−q

INTRODUCTION

It is well known that off-shell Green's functions depend in general on the gauge-fixing procedure used to quantize the theory, and in particular on the gauge-fixing parameter (GFP) chosen within a given scheme. A celebrated exception to this general fact is the vacuum polarization of the photon in QED, which is both gauge invariant (i.e., transverse) and GFP independent to all orders in perturbation theory. In contrast, the fermion self-energy $\Sigma(p)$ is GFP dependent already at the one-loop level. The dependence on the GFP is in general nontrivial and affects the properties of a given Green's function. In the framework of the covariant gauges, for example, depending on the choice of the GFP ξ, one may eliminate the ultraviolet divergence of the one-loop electron propagator $\Sigma(p,\xi)$ by choosing the Landau gauge $\xi=0$, or the infrared divergence appearing after on-shell renormalization by choosing the Yennie-Fried gauge $\xi=3$. The situation becomes even more complicated in the case of non-Abelian gauge theories, where all Green's functions depend on the GFP. Of course, when forming observables the gauge dependences of the Green's functions cancel among each other order by order in perturbation theory, due to powerful field-theoretical properties, a fact which reduces their seriousness. However, these dependences pose a major difficulty when one attempts to extract physically meaningful information from individual Green's functions. This is the case in at least two important situations, which both lie beyond the confines of fixed order perturbation theory: first, the Schwinger-Dyson (SD) equations, which constitute one of the few methods for obtaining nonperturbative information in the continuum; second, resonant transition amplitudes, where the taming of the physical kinematic singularity necessitates a resummation, which amounts to a nontrivial reorganization of the perturbative series.

In the context of the two nonperturbative situations mentioned above the fermion propagator is of particular interest. In the former case, the SD equation involving fermion propagators (self-energies) has an extended range of applications, most of which are linked to the mechanism of dynamical mass generation, which is explored by looking for nontrivial solutions to gap equations. The study of such equations has been particularly popular in QED [1], and even more so in QCD [2], where it has been intimately associated with the mechanism that breaks the chiral symmetry. Similar equations are relevant in QED_3, where the infrared regime of the theory is probed for a nontrivial fixed point [3], for technicolor models [4], gauged Nambu–Jona-Lasinio models [5], and more recently color superconductivity [6]. A similar quest takes place in top-color models, where the mass of the top quark is generated through a gap equation involving a strongly interacting massive gauge field [7]. The usual problem with the SD approach in general [8,9] and the gap equations in particular [10] is that sooner or later one is forced to choose a gauge, resorting to a variety of arguments, but gauge choices cast in general doubts on the robustness of the conclusions thusly reached. In the latter case, i.e., the resonant production of fermions, and in particular top quarks, one makes use of the resumed off-shell quark self-energy. Even though exactly at the resonance the gauge dependences cancel, infinitesimally away from it they persist, giving rise to artifacts obscuring the notion of the running width and the implementation of perturbative unitarity in the resulting Born-improved amplitudes [11].

It is known that gauge-invariant and GFP-independent effective off-shell Green's functions can be constructed by resorting to the pinch technique (PT) [12]. The PT reorganizes systematically a given physical amplitude into subampli-

*Email address: Daniele.Binosi@uv.es
†Email address: Joannis.Papavassiliou@uv.es

tudes, which have the same kinematic properties as conventional *n*-point functions (propagators, vertices, boxes) but, in addition, are endowed with desirable physical properties. Most importantly, at one-loop order (i) they are independent of the GFP, (ii) they satisfy naive (ghost-free), tree-level Ward identities (WI), instead of the usual Slavnov-Taylor identities [13], (iii) they contain only physical thresholds and satisfy very special unitarity relations [14], and (iv) they coincide with the conventional *n*-point functions when the latter are computed in the background field method Feynman gauge [15]. These properties are realized diagrammatically, by exploiting the elementary WI's of the theory in order to enforce crucial cancellations. The extension of the PT to two-loops has only recently been accomplished in the case of massless Yang-Mills theories such as QCD [16]. The studies presented so far in the literature have mainly focused on the general construction of the effective gauge-independent gluon self-energy, but little has been said about the fermion propagator [17–19].

Throughout the two-loop analysis of [16] it has been assumed that one can work without loss of generality in the covariant (renormalizable) Feynman gauge, i.e., begin the analysis by choosing the Feynman gauge when writing down the Feynman diagrams contributing to the *S* matrix. Of course, there is no doubt that the entire *S* matrix written in the Feynman gauge is equal to the same entire *S* matrix written in any other gauge. What is less obvious is that all relevant cancellations proceed without need of carrying out integrations over the virtual loop momenta, thus maintaining the kinematic identity of the various Green's functions intact, a point of crucial importance within the PT philosophy. As has been shown by explicit calculations (see, for example, [17]), this is indeed the case at one loop. Assuming that this important property persists at two loops, the highly nontrivial issue which was resolved in [16] was how the splitting of the three-gluon vertices appearing in the two-loop diagrams should proceed. We shall not review this point further, given that it has been exhaustively treated in [16]; here it should suffice to say that no such splitting should take place for the internal three-gluon vertices appearing inside the two-loop fermion propagator, or any other diagram for that matter. Therefore, one of the conclusions presented in [16], under the aforementioned assumption, was that the gauge-independent two-loop quark propagator in the presence of QCD interactions *coincides* with the conventional one computed in the Feynman gauge. In this paper we will verify this assumption in the cases of QED and QCD for the two-loop fermion self-energy.

In the first part of this paper we will track down the gauge cancellations systematically, and provide a simple diagrammatic algorithm which allows one to follow easily their implementation.[1] The key observation, which will be used as the only guiding principle throughout the intermediate steps, is that all contributions originating from the longitudinal parts of gauge boson propagators, by virtue of the WI they trigger, give rise to *unphysical* effective vertices, i.e., vertices which do not exist in the original Lagrangian. All such vertices cancel *diagrammatically* inside ostensibly gauge-invariant quantities, such as current correlation functions or *S*-matrix elements.[2] The final calculational recipe resulting from this analysis is that one can use directly the covariant Feynman gauge, which of course happens to be the simplest operationally. It is important to emphasize that exactly the same result is obtained even in the context of the noncovariant axial gauges, for example [21], where the Feynman gauge cannot be reached *a priori* by simply fixing appropriately the value of the gauge fixing parameter. Thus, even if one uses a bare gluon propagator of the general axial gauge form, after the aforementioned cancellations have taken place one arrives effectively to the answer written in the covariant Feynman gauge. Also notice that in calculating the final answer (something we shall not do here) one never has to carry out any of the tricky integrals characteristic of the axial gauges, i.e., integrals with unphysical poles of the form $n \cdot k$ [22].

The second part of the paper is devoted to the absorptive derivation of the same results. The absorptive construction exploits the unitarity and analyticity properties of physical amplitudes, together with the fundamental WI satisfied by *entire* physical processes dictated by the Becchi-Rouet-Stora (BRS) symmetry [23]. The salient points of this general method have been presented in detail in [24]. Here we will apply it to the case of the two-loop quark self-energy containing QED or QCD corrections.

The paper is organized as follows. In Sec. I we review the one-loop construction in both the QED and QCD. This will allow us to fix the notation and introduce in a simplified setting the diagrammatic algorithm used throughout the paper. In particular we will discuss how the gauge cancellations are achieved both in current correlation functions as well as in physical on-shell processes, such as $\gamma Q \to \gamma Q$ or $GQ \to GQ$, where Q is a quark and G a gluon. In Sec. II we tackle the two-loop case. The procedure is carried out in full detail, beginning from the same current correlation function as in the one-loop case. By means of a systematic, albeit lengthy analysis, we demonstrate explicitly all relevant cancellations, and finally define the GFP-independent two-loop electron (quark) self-energy for QED and QCD. We then turn to the description of how one may construct the PT effective Green's functions using unitarity and analyticity arguments. Thus, we first review the one-loop absorptive construction in both the Abelian and non-Abelian gauge theories (Sec. III), and introduce the notation which will be used in Sec. IV, where we will carry out in detail the full absorptive construction both in the QED and QCD frameworks. Finally, in Sec. V we present our concluding remarks.

[1] Some aspects of the cancellation mechanism described in this paper are similar in spirit to that presented in [20]; however, we do not resort to ''color orientation'' techniques.

[2] Given that the vertices involved are unphysical, one might be tempted to directly discard all such contributions by hand, instead of cancelling them algebraically against each other, as we do in the paper. In the case we consider here this seemingly *ad hoc* procedure would furnish the correct answer, but it is not known to us if it would work in general.

I. THE ONE-LOOP CASE

Before venturing into the intricacies of the two-loop construction, which is the main topic of this paper, we will first present the one-loop case, in an attempt to fix the ideas and the notation. In this section we will explain in detail the method which gives rise to effective, gauge-independent fermion self-energies. In particular, after setting up the diagrammatic notation which will be used throughout the paper, we will illustrate how the procedure works in the case of QED and QCD. The results for the one-loop case have already been presented in [16], albeit from a slightly different point of view; here we will recast them in the diagrammatic language introduced below, thus setting up the stage for the two-loop derivation. It turns out that in the one-loop case the difference between the Abelian (QED) and non-Abelian (QCD) constructions is purely group theoretical, and therefore a unified presentation will be followed; this will cease being the case at two loops.

We will assume that the theory has been gauge fixed by introducing in the gauge-invariant Lagrangian a gauge-fixing term of the form $(1/2\xi)(\partial_\mu A^\mu)^2$, i.e., a linear, covariant gauge; the parameter ξ is the GFP. This gauge-fixing term gives rise to a bare gauge-boson propagator of the form

$$\Delta_{\mu\nu}(\ell,\xi)=-\frac{i}{\ell^2}\left[g_{\mu\nu}-(1-\xi)\frac{\ell_\mu\ell_\nu}{\ell^2}\right] \tag{1.1}$$

which explicitly depends on ξ. The trivial color factor δ_{ab} appearing in the (gluon) propagator has been suppressed. The form of $\Delta_{\mu\nu}(\ell,\xi)$ for the special choice $\xi=1$ (Feynman gauge) will be of central importance in what follows; we will denote it by $\Delta^F_{\mu\nu}(\ell)$; i.e.,

$$\Delta_{\mu\nu}(\ell,1)\equiv\Delta^F_{\mu\nu}(\ell)=-\frac{i}{\ell^2}g_{\mu\nu}. \tag{1.2}$$

$\Delta_{\mu\nu}(\ell,\xi)$ and $\Delta^F_{\mu\nu}(\ell)$ will be denoted graphically as follows:[3]

For the diagrammatic proofs that will follow, in addition to the propagators $\Delta_{\mu\nu}(\ell)$ and $\Delta^F_{\mu\nu}(\ell)$ introduced above, we will need six auxiliary propagatorlike structures, as shown here:

All of these six structures will arise from algebraic manipulations of the original $\Delta_{\mu\nu}(\ell)$. For example, in terms of the above notation we have the following simple relation (we will set $\lambda\equiv\xi-1$):

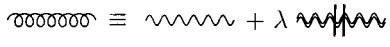

We next turn to the study of the gauge dependence of the fermion self-energy (electron in QED, quarks in QCD). The inverse electron propagator of order n in the perturbative expansion has the form (again suppressing color)

$$S_n^{-1}(p,\xi)=\not{p}-m-\Sigma^{(n)}(p,\xi), \tag{1.3}$$

where $\Sigma^{(n)}(p,\xi)$ is the nth order self-energy. Clearly $\Sigma^{(0)}=0$, and $S_0^{-1}(p)=\not{p}-m$. The quantity $\Sigma^{(n)}(p,\xi)$ depends explicitly on ξ already for $n=1$. In particular,

$$\Sigma^{(1)}(p,\xi)=\int[d\ell]\gamma^\mu S_0(p+\ell)\gamma^\nu\Delta_{\mu\nu}(\ell,\xi)$$

$$=\Sigma^{(1)}_F(p)+\lambda\Sigma^{(1)}_L(p) \tag{1.4}$$

with

$$\Sigma^{(1)}_F(p)\equiv\Sigma^{(1)}(p,1)=\int[d\ell]\gamma^\mu S_0(p+\ell)\gamma^\nu\Delta^F_{\mu\nu}(\ell) \tag{1.5}$$

and

$$\Sigma^{(1)}_L(p)=-S_0^{-1}(p)\int\frac{[d\ell]}{\ell^4}S_0(p+\ell)\gamma^\nu\ell_\nu$$

$$=-\int\frac{[d\ell]}{\ell^4}\ell_\mu\gamma^\mu S_0(p+\ell)S_0^{-1}(p)$$

$$=S_0^{-1}(p)\int\frac{[d\ell]}{\ell^4}S_0(p+\ell)S_0^{-1}(p)$$

$$-S_0^{-1}(p)\int\frac{[d\ell]}{\ell^4}. \tag{1.6}$$

In the above formulas $[d\ell]\equiv g^2\mu^{2\epsilon}[d^D\ell/(2\pi)^D]$ with

[3]For convenience, in our diagrammatic notation we will remove all factors of i appearing in the fermionic or bosonic propagators; they can be easily recovered as a global coefficient multiplying the Feynman diagram under consideration.

$D=4-2\epsilon$ the dimension of space-time, μ the 't Hooft mass,[4] and g the gauge coupling ($g\equiv e$ for QED, and $g\equiv g_s$ for QCD). The subscripts "F" and "L" stand for "Feynman" and "longitudinal," respectively. Notice that $\Sigma_L^{(1)}$ is proportional to $S_0^{-1}(p)$ and thus vanishes "on shell." The most direct way to arrive at the results of Eq. (1.6) is to employ the fundamental WI,[5]

$$\not{\ell}=S_0^{-1}(p+\not{\ell})-S_0^{-1}(p), \tag{1.7}$$

which is triggered every time the longitudinal momenta of $\Delta_{\mu\nu}(\ell,\xi)$ gets contracted with the appropriate γ matrix appearing in the vertices. Diagrammatically, this elementary WI gets translated to

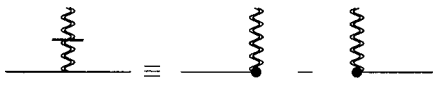

Then, the diagrammatic representation of Eqs. (1.4), (1.5), and (1.6) will be given by

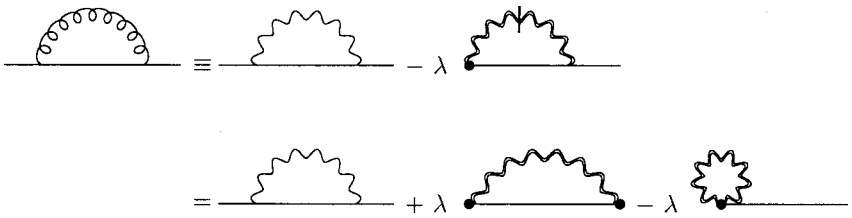

(1.8)

When considering physical amplitudes, the characteristic structure of the longitudinal parts established above allows for their cancellation against identical contributions originating from diagrams which are kinematically different from fermion self-energies, such as vertex graphs or boxes, *without* the need for integration over the internal virtual momenta. This last property is important because in this way the original kinematical identity is guaranteed to be maintained; instead, loop integrations generally mix the various kinematics. Diagrammatically, the action of the WI is very distinct: it always gives rise to unphysical effective vertices, i.e., vertices which do not appear in the original Lagrangian; all such vertices cancel in the full, gauge-invariant amplitude.

To actually pursue these special cancellations explicitly one may choose among a variety of gauge-invariant quantities. For example, one may consider the current correlation function $I_{\mu\nu}$ defined as (in momentum space)

$$I_{\mu\nu}(q)=i\int d^4x\, e^{iq\cdot x}\langle 0|T[J_\mu(x)J_\nu(0)]|0\rangle$$

$$=(g_{\mu\nu}q^2-q_\mu q_\nu)I(q^2), \tag{1.9}$$

where the current $J_\mu(x)$ is given by $J_\mu(x)=:\bar{Q}(x)\gamma_\mu Q(x):$. Of course, $I_{\mu\nu}(q)$ coincides with the photon vacuum polarization of QED. Equivalently, one may study physical on-shell processes such as $\gamma e\to\gamma e$, $\gamma Q\to\gamma Q$, or $GQ\to GQ$, where G is a gluon. Of these three processes the first two are the most economical, since in the latter the algebra is more complicated due to the appearance of three gluon vertices.

To see explicitly the mechanism enforcing these cancellations in the QED and QCD cases, we first consider the one-loop photonic or gluonic corrections, respectively, to the quantity $I_{\mu\nu}$. Clearly either set of corrections is GFP independent, since the current $J_\mu(x)$ is invariant under both the $U(1)$ and the $SU(3)$ gauge transformations

$$\begin{aligned} Q(x)&\to\exp\{-i\theta(x)\}Q(x),\\ Q(x)&\to\exp\{-i\theta_a(x)T^a\}Q(x),\\ \bar{Q}(x)&\to\exp\{i\theta(x)\}\bar{Q}(x),\\ \bar{Q}(x)&\to\exp\{i\theta_a(x)T^a\}\bar{Q}(x), \end{aligned} \tag{1.10}$$

where $T^a=\frac{1}{2}\lambda^a$, with λ^a the Gell-Mann matrices.

The relevant diagrams are those shown in Fig. 1. To see the appearance of the unphysical vertices, we carry out the manipulations presented in Eqs. (1.4), (1.5), and (1.6), or, equivalently, in Eq. (1.8), this time embedded inside $I_{\mu\nu}(q)$. Thus, from diagrams (b) and (c) we arrive at

[4]Throughout the paper we use $\int[d\not{\ell}]/\ell^2=0$ and $\int[d\not{\ell}]\not{\ell}_\alpha\not{\ell}_\beta/\ell^4=g_{\alpha\beta}D^{-1}\int[d\not{\ell}]/\ell^2=0$, valid in dimensional regularization. In addition, integrals odd in the integration variable are considered to vanish. Notice, however, that nowhere will we use the slightly subtler $\int[d\not{\ell}]/\ell^4=0$, which is often employed in the literature.

[5]A formal derivation of the gauge dependence may be obtained by resorting to the so-called Nielsen identities [25].

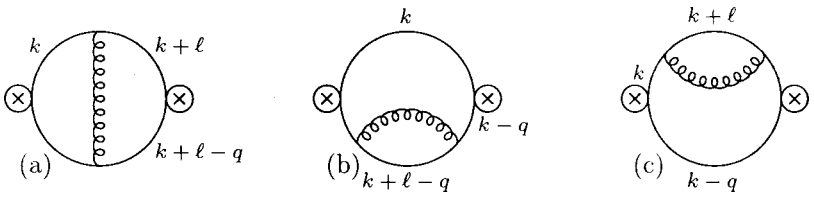

FIG. 1. One-loop diagram contributing to the QED/QCD fermion self-energy.

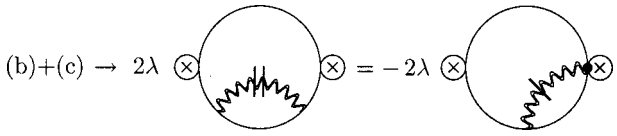

We thus see that since the action of the elementary WI of Eq. (1.7) amounts to the cancellation of internal propagators, its diagrammatic consequence is that of introducing an unphysical effective vertex, describing an interaction of the form $\gamma\gamma\bar{Q}Q$ or $\gamma G\bar{Q}Q$, depending on whether we consider photonic or gluonic corrections. This type of vertex may be depicted by means of a Feynman rule of the form

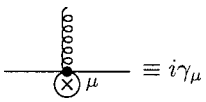

μ being the index of the external current.

To see how the above unphysical contributions cancel inside $I_{\mu\nu}$ we turn to diagram (a). The action of the WI may be translated to the following diagrammatic picture:

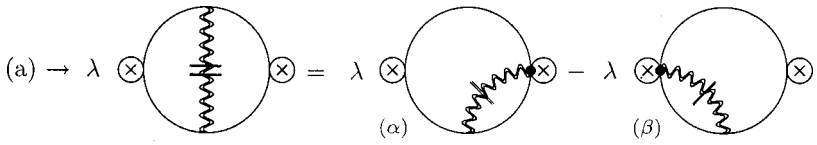

It is then elementary to establish that the two diagrams on the right-hand side of the above diagrammatic equation add up. Indeed, for (α) we have (suppressing the integral measure)

$$(\alpha)\sim\lambda\mathrm{Tr}\left[\gamma^{\mu}\frac{1}{\not k-m}\gamma^{\nu}\frac{1}{\not k+\not\ell-\not q-m}\times\gamma^{\rho}\frac{1}{\not k-\not q-m}\right]\frac{\ell_{\rho}}{\ell^{4}},\tag{1.11}$$

whereas from (β), taking the trace counter-clockwise and using the fact that $I_{\mu\nu}$ is symmetric under the exchange $\mu\leftrightarrow\nu$, we obtain[6]

$$(\beta)\sim-\lambda\mathrm{Tr}\left[\gamma^{\nu}\frac{1}{\not k+\not\ell-m}\gamma^{\mu}\frac{1}{\not k-\not q-m}\times\gamma^{\rho}\frac{1}{\not k+\not\ell-\not q-m}\right]\frac{\ell_{\rho}}{\ell^{4}}$$

$$\overset{\substack{k+\ell\to k\\ \ell\to-\ell\\ \mu\leftrightarrow\nu}}{=}\lambda\mathrm{Tr}\left[\gamma^{\mu}\frac{1}{\not k-m}\gamma^{\nu}\frac{1}{\not k+\not\ell-\not q-m}\times\gamma^{\rho}\frac{1}{\not k-\not q-m}\right]\frac{\ell_{\rho}}{\ell^{4}}.\tag{1.12}$$

Summing the two equations above then, it is clear how the gauge-dependent part of the one-loop amplitude cancels altogether. Having proved that the GFP-dependent contributions coming from the original graphs containing $\Sigma^{(1)}(p,\xi)$, i.e., Fig. 1(b) and Fig. 1(c) cancel exactly against equal but opposite *propagatorlike* contributions coming from Fig. 1(a), one is left with the ''pure'' GFP-independent one-loop fermion self-energy, $\hat{\Sigma}^{(1)}(p)$. Clearly, it concides with the $\Sigma_F^{(1)}(p)$ of Eq. (1.5), i.e., [17]

$$\hat{\Sigma}^{(1)}(p)=\Sigma_F^{(1)}(p).\tag{1.13}$$

Next, we will consider the physical process $\gamma Q\to\gamma Q$ in order to analyze how the procedure outlined above works in the case of an *S*-matrix element. The one-loop diagrams for the process under consideration are listed in Fig. 2. We will isolate the parts of the above diagrams proportional to λ,

[6]Throughout the paper we will make extensive use of suitable shiftings of the integration variables together with various rearrangements of seemingly distinct diagrams.

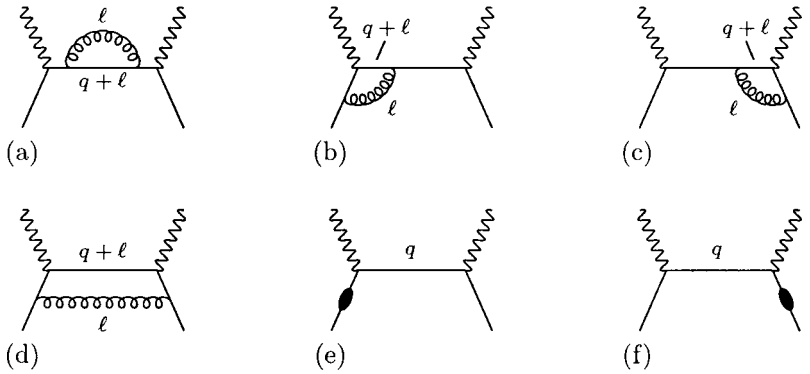

FIG. 2. One-loop QED/QCD correction to the process $\gamma Q \to \gamma Q$ $(p_1+p_2=q=p_3+p_4)$. Diagrams (e) and (f) correspond to the (one-loop) renormalization of the external legs.

using again the WI of Eq. (1.8), together with the fact that the external particles are on their mass shell. We emphasize that the point of this exercise is not to prove the GFP independence of the S matrix, but rather to recognize that the GFP cancellations proceed in a very special way: the λ-dependent parts of vertices [(b), (c)] and boxes [(d)] do not maintain the same kinematic identity as their parent graphs; instead, they reduce to simpler kinematic structures, which are precisely those stemming from the original propagator diagram (a), and finally cancel algebraically against each other.

To see this in detail, we begin with diagram (a); applying the identity of Eq. (1.8) in a symmetric way, i.e., allowing the longitudinal parts to act once on the left and once on the right vertex of the diagram, one obtains the following GFP-dependent part:

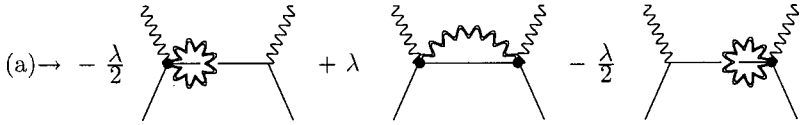

Similarly, we find

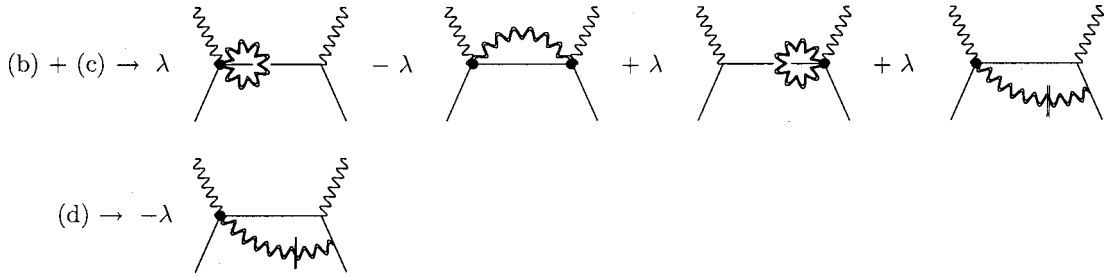

Thus we see that the GFP-dependent part of the box diagram (d) completely cancels against the last diagram appearing in the above equation, in such a way that, after adding everything up, we get

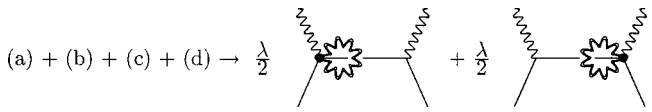

The remaining tadpolelike contributions will actually cancel against the GFP-dependent parts of the diagrams (e) and (f), representing the renormalization of the external legs. The renormalization constant reads

$$Z_2^{1/2}=1+\frac{1}{2}\delta Z_2+\cdots, \tag{1.14}$$

where δZ_2 represents the one-loop counterterm in the pertur-

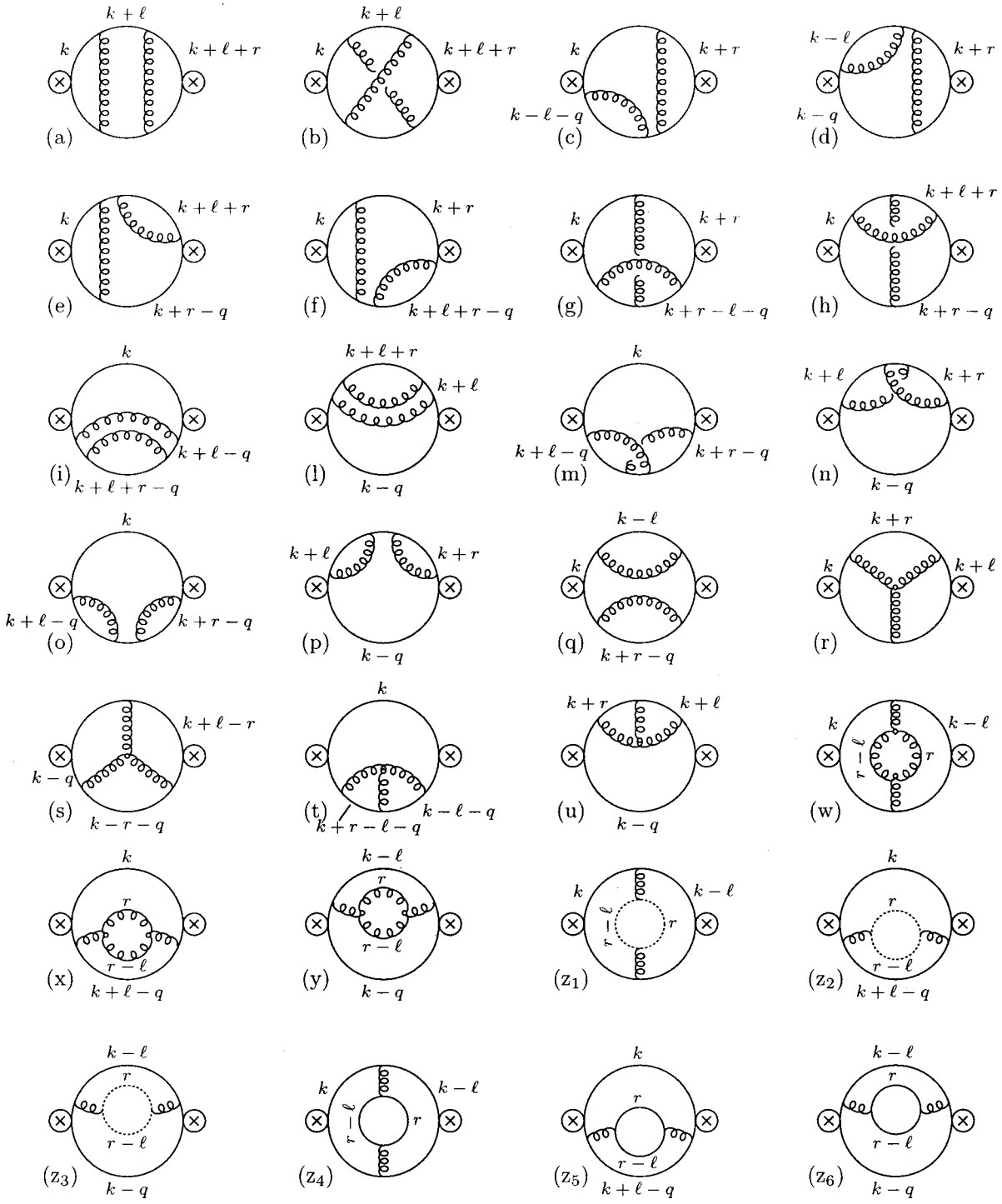

FIG. 3. Two-loop diagram contributing to the QCD fermion self-energy.

bative expansion; in the on-shell renormalization scheme it is defined as

$$\delta Z_2 = \frac{\partial}{\partial \not{p}} \Sigma^{(1)}(p,\xi)\Big|_{\not{p}=m} = \frac{\partial}{\partial \not{p}} \left[\Sigma_F^{(1)}(p) + \lambda \Sigma_L^{(1)}(p) \right]\Big|_{\not{p}=m} \quad (1.15)$$

We next focus our attention on the $\Sigma_L^{(1)}$ part of Eq. (1.15). As can be seen from Eq. (1.6), $\Sigma_L^{(1)}(p)$ is of the form

$$\Sigma_L^{(1)}(p) \equiv (\not{p}-m) g(\not{p}) (\not{p}-m) + (\not{p}-m) c, \quad (1.16)$$

where c is a momentum-independent constant (see footnote 4); thus

$$\Sigma_L^{(1)}(p)|_{\not p=m}=0, \quad \delta Z_{2L}=\lambda c. \tag{1.17}$$

Diagrammatically then, Eq. (1.8) implies that

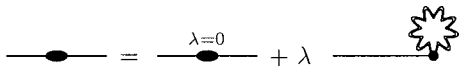

where the right-hand side is evaluated at $\not p=m$. Thus, recalling the extra 1/2 factor appearing in Eq. (1.14), the GFP-dependent part of the wave-function renormalization diagrams is given by

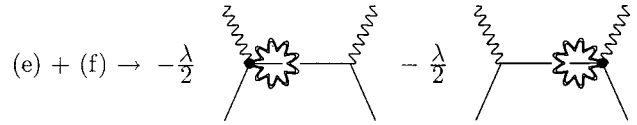

which completes the proof that the GFP independence of the *S*-matrix element is implemented in the kinematically distinct way advocated above. Again, the remaining pure GFP-independent fermion self-energy which survives is simply the one given in Eq. (1.13).

II. THE TWO-LOOP CASE

In the previous section we set up the general method for treating the GFP-dependent contributions associated with the longitudinal momenta of the gauge bosons propagators inside Feynman graphs, studied at the one-loop level, the special cancellation mechanism that this implies. Thus we have been able to define the one-loop GFP-independent fermion self-energy $\hat{\Sigma}^{(1)}(p)$. In this section we proceed to the main subject of this paper, namely the two-loop definition of the GFP-independent fermion self-energy.

At the two-loop level the presence of up to three gauge boson propagators in the internal fermion loop will give rise to $O(\lambda^3)$, $O(\lambda^2)$, and $O(\lambda)$ GFP-dependent pieces. Of course, the gauge cancellations proceed independently at each order in λ, a fact which facilitates the identification of diagrams (or parts of diagrams) which can mix with each other. Notice, however, that occasionally we will deviate from this elementary rule of thumb, in order to exploit the fact that one can identify massive cancellations between different diagrams *before* separating out the different orders in the GFP λ; this happens, for example, in the Abelian-like part of the gauge cancellation, as we will see below. We will now proceed to the detailed analysis of the two-loop construction, showing first how it works in the Abelian (QED) case, and concentrating then on the non-Abelian case (QCD).

A. Abelian case

The diagrams contributing to this part of the amplitude are the ones denoted (a),...,(q) in Fig. 3.[7] In this part of the cancellation one can carry out massive cancellations dealing with $O(\lambda^2)$ and $O(\lambda)$ diagrams at the same time, by pinching with only one propagator, while letting the other one untouched. We will now consider in detail a couple of these diagrams showing how the procedure works in the two-loop case.

From the box diagram (a) we get, for example, the following equation:

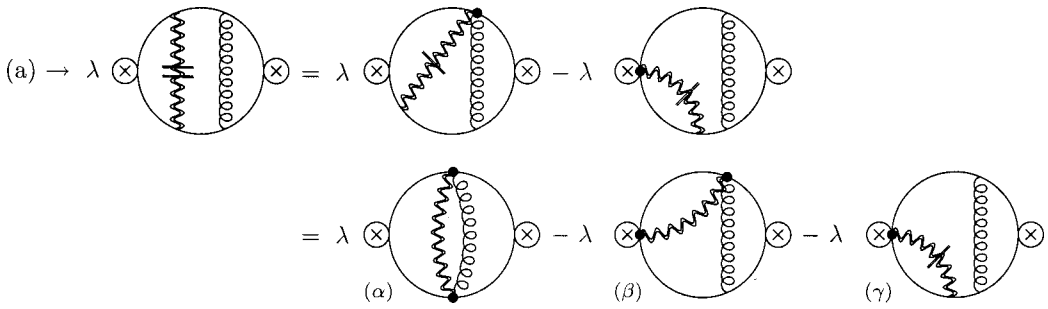

Let us concentrate on the three topologies shown above. It is clear that topology (α) can be generated *only* from diagram (b), and so it must cancel against it. Topologies (β) and (γ) will be also generated from diagrams (d) and (c); however, these last two diagrams do not need to cancel in full against the one coming from (d) and (c), because, as we will see, topologically analogous contributions will also appear from other diagrams.

As a second example, we consider the box diagram (b), which gives

[7]Diagrams (z_4), (z_5) and (z_6) can be put in the Feynman gauge right from the start, due to the transversality of the fermionic sector of the photon/gluon propagator (see also Sec. II B).

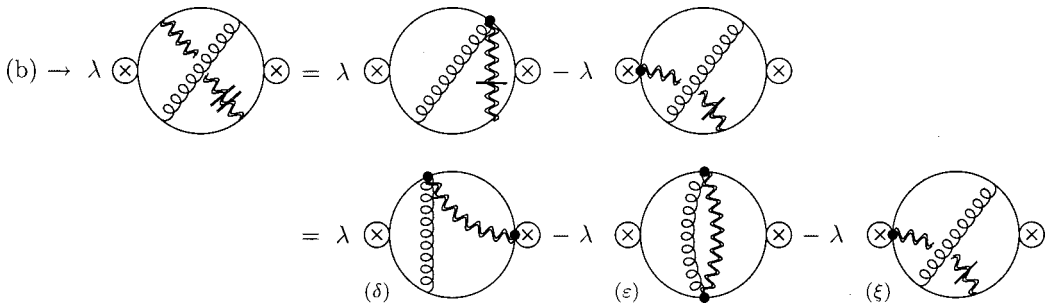

As expected, topology (ϵ) cancels against the diagram (α) of the previous equation (after exchanging the order of the internal lines and relabeling the internal momenta), but we have generated also two new topologies: (δ) which will be generated as well by diagram (e), and (ζ) which will be generated by (g). Letting untouched the vertical propagator in diagrams (c),...,(h), we then arrive at the following equation:

$$(a)+(b)+(c)+(d)+(e)+(f)+(g)+(h)\rightarrow$$

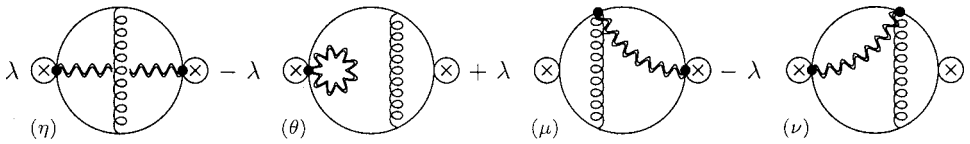

Actually the last two diagrams add up to zero. To see this, we can use their $\mu\leftrightarrow\nu$ symmetry, to observe that (the integral measures are suppressed)

$$(\mu)\sim\lambda\mathrm{Tr}\left[\gamma^{\mu}\frac{1}{\not k-m}\,\gamma^{\rho}\frac{1}{\not k+\not r+\not\ell-m}\,\gamma^{\nu}\frac{1}{\not k+\not r-\not q-m}\,\gamma^{\sigma}\frac{1}{\not k-\not q-m}\right]\Delta_{\rho\sigma}(r^2)\,\frac{1}{\ell^4}, \tag{2.1}$$

while

$$(\nu)\sim-\lambda\mathrm{Tr}\left[\gamma^{\nu}\frac{1}{\not k+\not\ell+\not r-m}\,\gamma^{\rho}\frac{1}{\not k-m}\,\gamma^{\mu}\frac{1}{\not k+\not\ell-\not q-m}\,\gamma^{\sigma}\frac{1}{\not k+\not\ell+\not r-\not q-m}\right]\Delta_{\rho\sigma}(r^2)\,\frac{1}{\ell^4}$$

$$\overset{k+\ell+r\rightarrow k}{=}-\lambda\mathrm{Tr}\left[\gamma^{\nu}\frac{1}{\not k-m}\,\gamma^{\rho}\frac{1}{\not k-\not\ell-\not r-m}\,\gamma^{\mu}\frac{1}{\not k-\not r-\not q-m}\,\gamma^{\sigma}\frac{1}{\not k-\not q-m}\right]\Delta_{\rho\sigma}(r^2)\,\frac{1}{\ell^4}$$

$$\overset{\substack{\ell\rightarrow-\ell\\ r\rightarrow-r\\ \mu\leftrightarrow\nu}}{=}-\lambda\mathrm{Tr}\left[\gamma^{\mu}\frac{1}{\not k-m}\,\gamma^{\rho}\frac{1}{\not k+\not r+\not\ell-m}\,\gamma^{\nu}\frac{1}{\not k+\not r-\not q-m}\,\gamma^{\sigma}\frac{1}{\not k-\not q-m}\right]\Delta_{\rho\sigma}(r^2)\,\frac{1}{\ell^4}. \tag{2.2}$$

Moreover, from the remaining diagrams we get

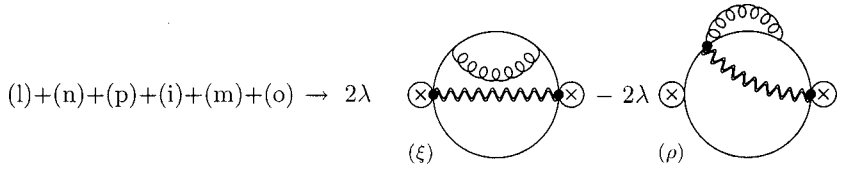

After having identified these cancellations of mixed order [$O(\lambda)$ and $O(\lambda^2)$] we next find it convenient to pursue the remaining cancellations treating separately the $O(\lambda)$ and $O(\lambda^2)$ GFP-dependent amplitudes.

1. The $O(\lambda^2)$ cancellation

For this case one has to replace the propagator

appearing in the diagrams (η),...,(ρ) with the propagator

It is then fairly easy to show that

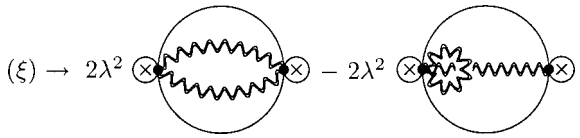

which implies

$$(\xi)+(\eta)=0. \tag{2.3}$$

Moreover, considering diagram (θ) we find the result

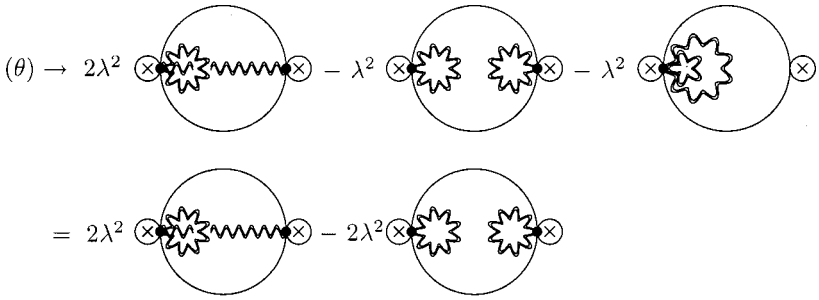

The fact that the last two diagrams in the first line of the previous equality can be added up reflects the freedom of moving at will the photon (gluon) tadpolelike loops in a given pinched diagram. This can be done because such loops represent scalar quantities—defined in Eq. (1.6)—with no interactions left at the vertex. Notice that this freedom does not interfere with our notion of unphysical vertices, since both diagrams, written in either way, are equally unphysical. We will often use this property in what follows.

Adding to the above result the contribution coming from diagram (q), we then get

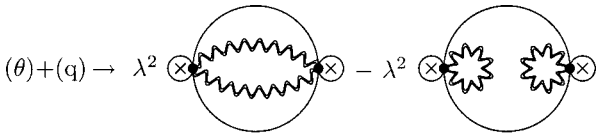

a combination that should then cancel completely with the diagram (ρ), which at $O(\lambda^2)$ reads

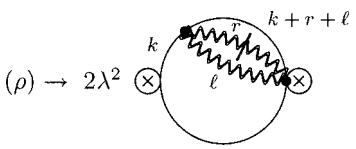

(2.4)

In order to make this cancellation manifest, we need to change the given topology by means of pinching internal fermion propagators. Of course, the only available momentum r in diagram (ρ) cannot pinch directly, due to the obvious kinematic mismatch. However, one has

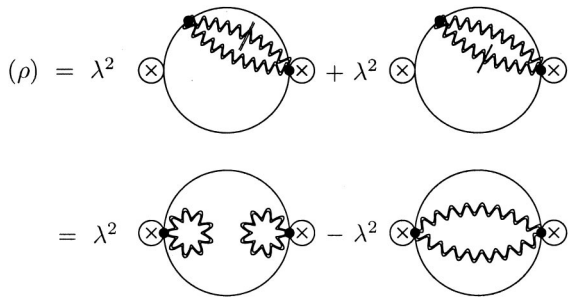

which implies finally

$$(\rho)+(\theta)+(\mathrm{q})=0. \tag{2.5}$$

2. The $O(\lambda)$ cancellation

For this case one has to replace the propagator

appearing in the diagrams (η),...,(ρ) with the Feynman propagator

However, these diagrams represent only half of those contributing to this order; clearly, the other half is obtained by inverting, with respect to the previous calculation, the pinching and Feynman propagators. For example, for the diagrams (c),...,(h) the new terms are obtained by pinching with the vertical propagator, treating the other one as the Feynman propagator. Now, notice that the topologies (η) and (θ) can be canceled only by these new contributions coming from the diagrams (a) and (b). In fact, one has

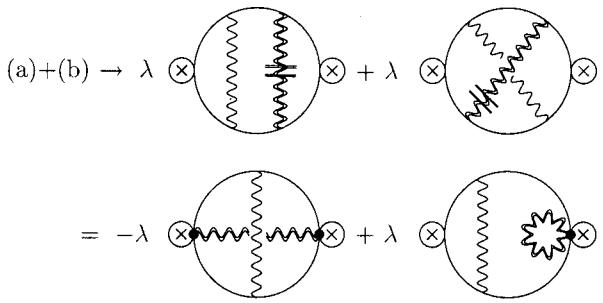

which are exactly the topologies needed to cancel the (η) and (θ) terms. In addition, the following new contributions are obtained from diagrams (c),...,(n):

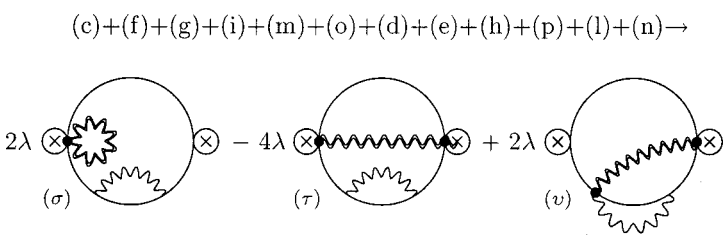

Finally, the two contributions coming from diagram (q) will add up giving the final result

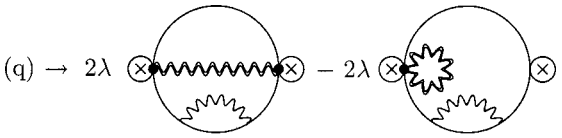

Adding all terms together, we finally find that

$$(\xi)+(\rho)+(\sigma)+(\tau)+(\upsilon)+(\mathrm{q})=0, \tag{2.6}$$

which completes the proof of the gauge cancellation in the Abelian case.

B. Non-Abelian case

We next proceed to address the non-Abelian case. With respect to the Abelian case we have two main differences: first, there are seven more diagrams (plus ghosts) to consider (see diagrams (r),....,(y) in Fig. 3), all of which contain at least one three-gluon vertex; second, due to the nontrivial color structure of the theory, the cancellations in the Abelian-like subset of graphs will not go through as before.

Let us first deal with this latter point. Taking into account the factors of *i* coming from the Feynman rules, we have the following color prefactors:

$$\begin{aligned}
&(\mathrm{a}),\ (\mathrm{c}),\ (\mathrm{d}),\ (\mathrm{e}),\ (\mathrm{f}),\ (\mathrm{i}),\ (\mathrm{l}),\ (\mathrm{o}),\ (\mathrm{p}),\ (\mathrm{q}) \sim -C_f^2,\\
&(\mathrm{b}),\ (\mathrm{g}),\ (\mathrm{h}),\ (\mathrm{m}),\ (\mathrm{n}) \sim -C_f^2+\tfrac{1}{2}C_A C_f,\\
&(\mathrm{r}),\ (\mathrm{s}),\ (\mathrm{t}),\ (\mathrm{u}) \sim \tfrac{1}{2}C_A C_f,\\
&(\mathrm{w}),\ (\mathrm{x}),\ (\mathrm{y}) \sim -\tfrac{1}{2}C_A C_f,
\end{aligned} \tag{2.7}$$

where C_f and C_A represent, respectively, the quadratic Casimir operators of the fundamental and the adjoint representations of the $SU(N_c)$ group, i.e.,

$$C_f^2=\frac{N_c^2-1}{2N_c}, \quad C_A=N_c. \tag{2.8}$$

It is then clear that, while for the parts of the Abelian-like diagrams (a),...,(q) which are proportional to C_f^2 the cancellations proven in the previous sections will still go through, the parts proportional to C_A will survive, and will eventually cancel against contributions from the purely non-Abelian graphs. Thus our first task is to determine the non-Abelian remainders of the diagrams appearing in the second line of Eq. (2.7), at each order in λ.

At any order in λ one has

$$(g)+(h)+(m)+(n) \rightarrow$$

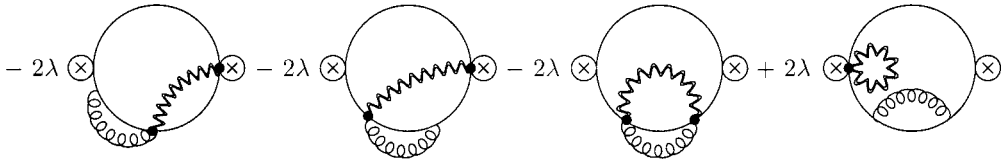

(2.9)

Now, at $O(\lambda^2)$ the above equation reads

$$(g)+(h)+(m)+(n) \rightarrow$$

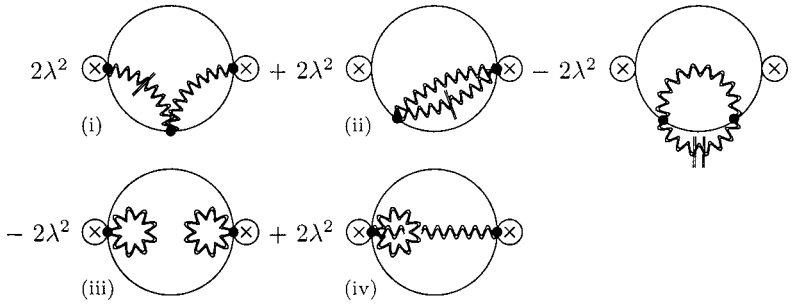

On the other hand,

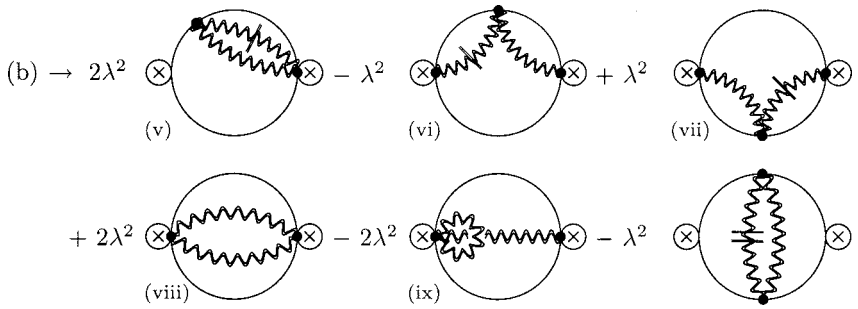

It is straightforward to verify, using the procedure presented following Eq. (2.4), that

$$(ii)+(iii)+(v)+(viii)=0,$$
$$(i)+(vi)+(vii)=0. \tag{2.10}$$

Finally, (iv) and (ix) cancel directly. Thus, at $O(\lambda^2)$ we are left with the non-Abelian remainder

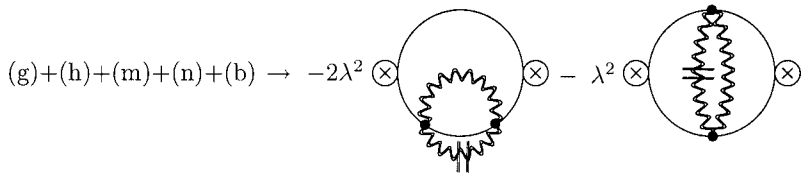

(2.11)

which will be canceled later.

In the $O(\lambda)$ case, we have to substitute the propagator

appearing in Eq. (2.9) with the Feynman propagator

Moreover, as already mentioned, we have still to compute the GFP-dependent contributions (linear in λ) of diagrams

(g), (h), (m), (n), where the Feynman and pinching propagators are reversed with respect to that presented in Eq. (2.9). Thus, we obtain:

(g)+(h)+(m)+(n) →

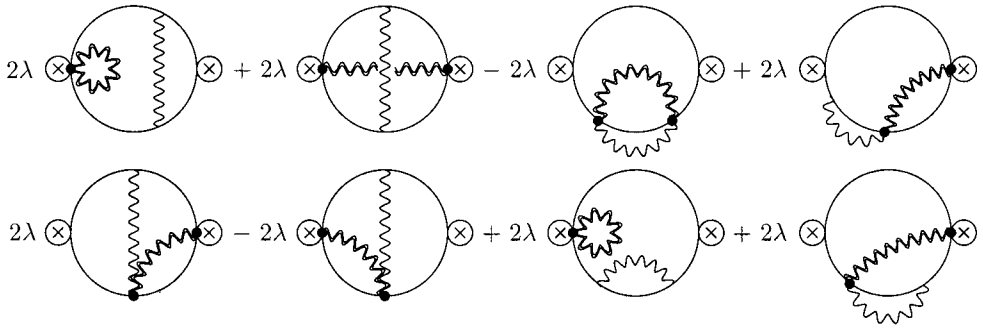

Finally, from (b) we obtain

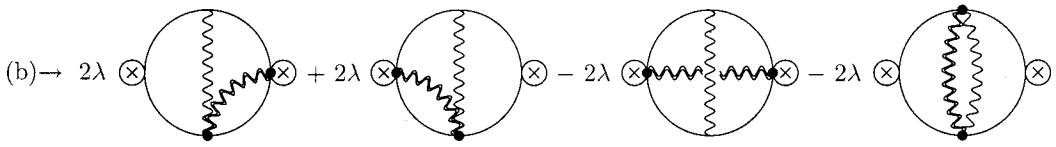

Thus, putting all terms together, we arrive at the $O(\lambda)$ non-Abelian remainder

(g)+(h)+(m)+(n)+(b) →

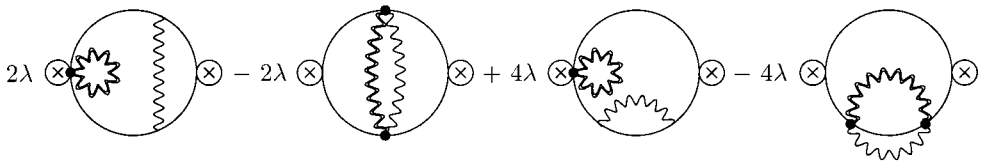

(2.12)

We next concentrate on the purely non-Abelian diagrams (q),..., (y). In this case we will split the calculation from the beginning into different orders in λ. Notice that the $O(\lambda^3)$ cancellation is automatically accomplished due to the elementary WI

$$k_1^\mu k_2^\nu k_3^\rho \Gamma_{\mu\nu\rho}(k_1,k_2,k_3)=0, \tag{2.13}$$

satisfied by the three-gluon vertex. Therefore we only have to collect $O(\lambda^2)$ and $O(\lambda)$ contributions.

1. The $O(\lambda^2)$ cancellation

In dealing with the non-Abelian diagrams, we have found it more economical to carry out all possible cancellations before letting the longitudinal momenta act on the three gluon vertex. Consider, for example the diagrams (r) and (s): each one gives rise to three possible $O(\lambda^2)$ diagrams, as shown below

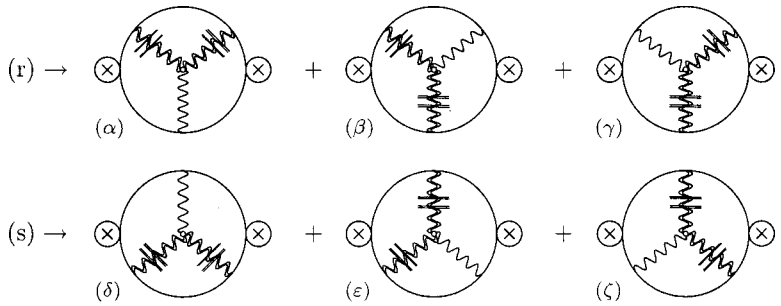

Similarly, the basic topologies obtained from diagrams (t) and (u) can be easily worked out. After some elementary manipulations involving further pinching in order to allow the combination/cancellation of seemingly different topologies (but without acting on the three-gluon vertex), one finally arrives at

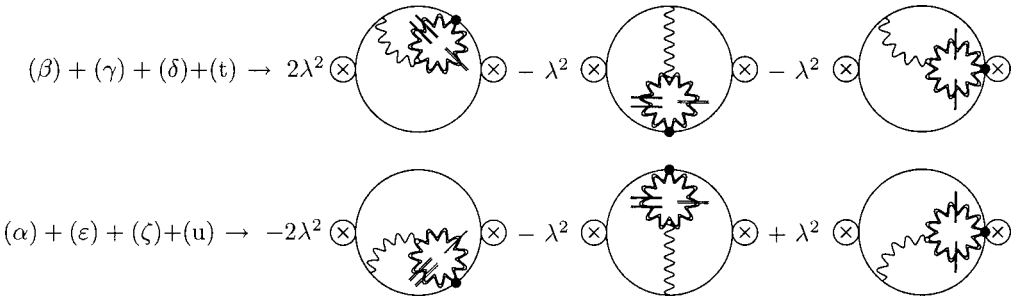

We next consider diagrams (w), (x), and (y), and the corresponding ghost and fermion diagrams $(z_1),\ldots,(z_6)$. Let us introduce the one-loop gluon self-energy

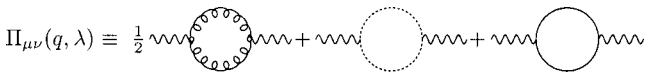

which, due to its transversality, satisfies

$$q^\mu \Pi_{\mu\nu}(q,\lambda)=0. \tag{2.14}$$

This fact will then imply that as far as the ghost and fermion diagrams $(z_1),\ldots,(z_6)$ are concerned, one can effectively fix the Feynman gauge $\lambda=0$ right from the start, while for the diagrams (w), (x), and (y) the above transversality condition has the consequence of putting the external propagators (i.e., those touching the fermion loop) in the Feynman gauge. Thus in these latter graphs the pinching momenta can act on the three gluon vertex *only*, triggering the elementary WI.

$$k_1^\mu k_2^\nu \Gamma_{\mu\nu\rho}(k_1,k_2,\ell)=-\tfrac{1}{2}\ell^2(k_1-k_2)_\rho + \tfrac{1}{2}\ell\cdot(k_1-k_2)\ell_\rho. \tag{2.15}$$

The first term represents an inverse propagator times a momentum which in general cannot pinch, whereas the second term represents an effective three gluon vertex times a pinching momentum. Thus, for example,

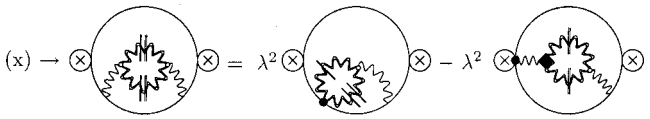

where we did not draw a tadpolelike diagram since it is zero upon integration in the internal momenta, and the black box represents the unphysical effective vertex defined in Eq. (2.15), i.e.,

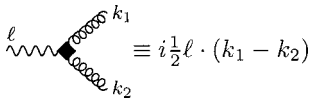

(2.16)

Proceeding in this way we find [recall that there is a relative minus sign between diagrams (r),..., (u) and (w),..., (y)]

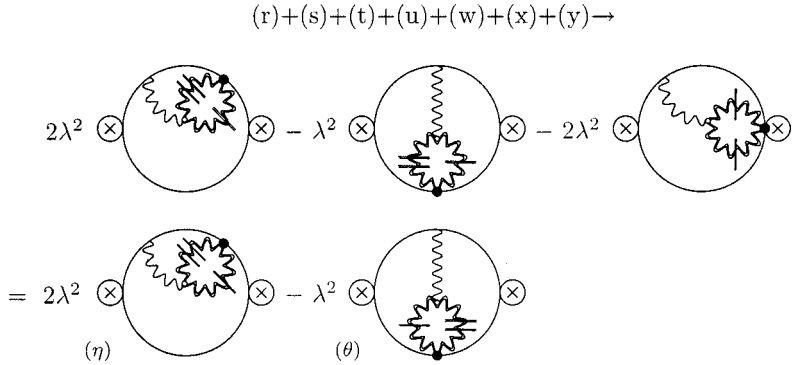

where the last step is achieved by allowing the second diagram in the first line to pinch further. The coefficient multiplying this equation is $C_f C_A/2$. Notice that the effective vertex introduced in Eq. (2.16) does not appear at this point.

We can finally act on the three gluon vertex with the remaining pinching momenta, to obtain

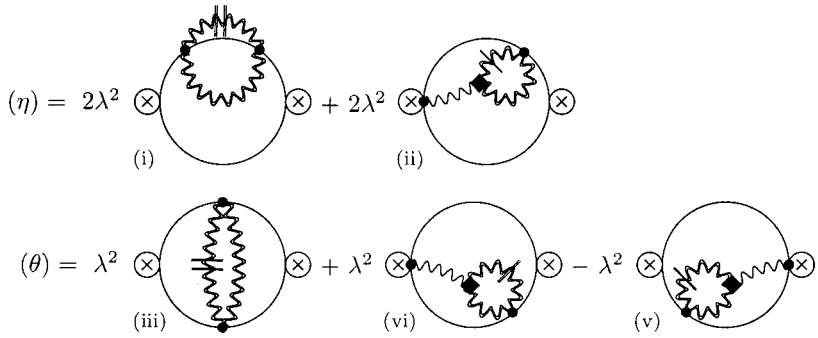

It is then clear how the final steps proceed: the combination (i) + (iii) cancels the $O(\lambda^2)$ non-Abelian remainder of Eq. (2.11), while, as can be easily shown

$$(\mathrm{ii})+(\mathrm{vi})+(\mathrm{v})=0. \tag{2.17}$$

This completes the proof of the cancellation of the $O(\lambda^2)$ terms.

2. The $O(\lambda)$ cancellation

As in the previous case, the strategy will be to achieve the widest possible cancellation between diagrams, avoiding to act on the three-gluon vertex. First of all, each one of the diagrams (s),..., (u) will again generate three contributions, which are obtained from the $O(\lambda^2)$ ones by trading one of the propagators

for a Feynman propagator. Then, taking all these diagrams into account, we arrive at the equation

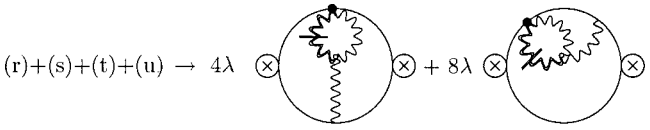

We are now left with the topologies (w),…,(z_3). As in the $O(\lambda^2)$ case, for the external propagators $\lambda=0$. However, contrary to the previous case where each one gave a single contribution, at $O(\lambda)$ each of the topologies (w), (x), and (y) gives rise to two equal contributions [hence the factor of 2 in Eq. (2.19)]. Moreover, for these diagrams the pinching momenta can only act on the three-gluon vertex, triggering the elementary WI

$$k_1^\mu \Gamma_{\mu\nu\rho}(k_1,k_2,\not\ell)=(\not\ell^2 g_{\nu\rho}-\not\ell_\nu \not\ell_\rho)-(k_2^2 g_{\nu\rho}-k_{2\nu}k_{2\rho}). \tag{2.18}$$

The first and third term of the above expression represent two inverse propagators in the Feynman gauge; the second and fourth terms contain instead two longitudinal momenta each, one acting on the external fermion loop, and the other one on the remaining three-gluon vertex. For example, considering diagram (w), we find

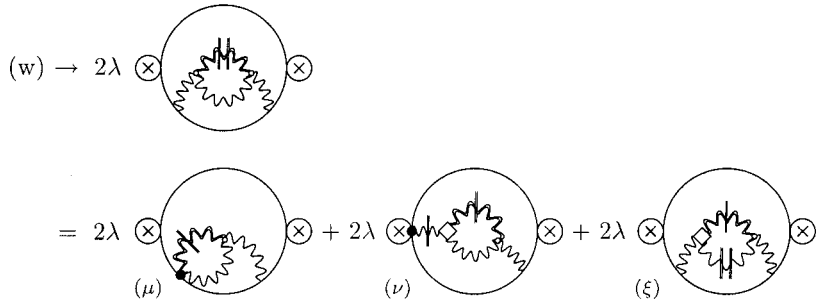

(2.19)

The diagram (μ) comes from the first term in Eq. (2.18), while the third term in the WI produces in this case a tadpolelike diagram which is odd in the integrated momentum and vanishes. The term (ν) and (ξ) are generated from the second and fourth term in Eq. (2.18), respectively. Notice that a new unphysical effective three-gluon vertex

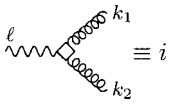

has appeared. After acting on the remaining three-gluon vertex of diagram (ξ) we get

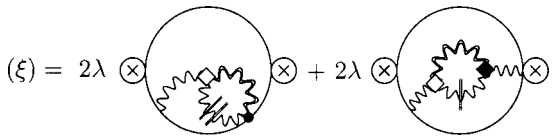

Proceeding in this way we arrive at the result

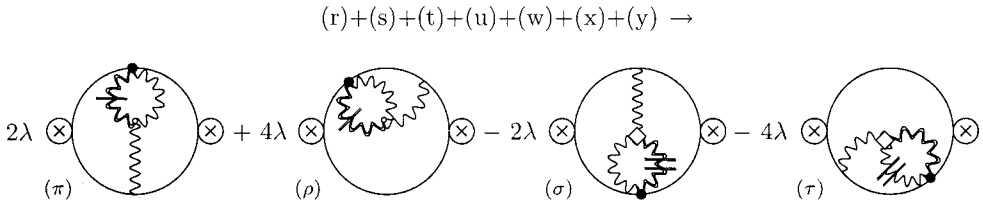

where the group-theoretical coefficient of this equation is $C_A C_f/2$.

The final step of the proof is achieved by acting on the three-gluon vertex in (ρ) and (π) with the remaining pinching momenta. One has, keeping in mind Eq. (2.18),

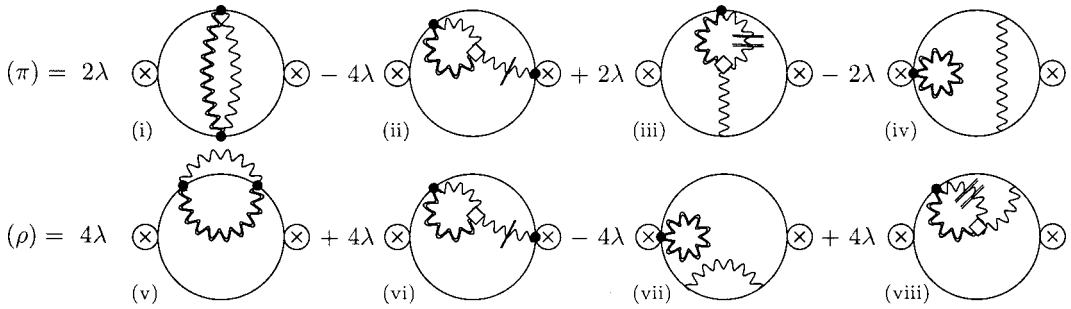

Then the sum (i)+(iv)+(v)+(vii) cancels against the $O(\lambda)$ non-Abelian remainder (2.12), (ii) and (vi) cancel directly, while finally

$$(\tau)+(\text{viii})=(\sigma)+(\text{iii})=0. \tag{2.20}$$

This completes the proof of the non-Abelian gauge cancellation.

We see that, as happened in the one-loop case, the GFP-dependent contributions coming from the original graphs of Fig. 3 defining $\Sigma^{(2)}(p,\xi)$, cancel exactly against equal but opposite *propagatorlike* contributions coming from vertex-like and boxlike graphs. Thus, one is left with the ''pure'' GFP-independent one-loop fermion self-energy, $\hat{\Sigma}^{(2)}(p)$, which again coincides with the $\Sigma_F^{(2)}(p) \equiv \Sigma^{(2)}(p,1)$, i.e.,

$$\hat{\Sigma}^{(2)}(p)=\Sigma_F^{(2)}(p), \tag{2.21}$$

which constitutes the central result of this paper.

III. THE ABSORPTIVE CONSTRUCTION: THE ONE-LOOP CASE

In the next two sections we will show in detail how one may construct the two-loop PT effective fermion self-energy using unitarity and analyticity arguments [24]. The general idea is the following: The imaginary parts of the two-loop PT fermion self-energies $\hat{\Sigma}^{(2)}$ of QED and QCD are related by the optical theorem to precisely identifiable and very special parts of four different cross sections. In particular, for the case of QED, the two-particle Cutkosky cuts of $\hat{\Sigma}^{(2)}$ are

related to the ''genuine'' *s*-channel part of the one-loop cross section for the process $\gamma Q \to \gamma Q$ while, at the same time, the three-particle Cutkosky cuts of the same quantity are related to the genuine *s*-channel parts of the tree-level cross sections for the processes $\gamma Q \to \gamma Q$, $\gamma Q \to Q\bar{Q}Q$, and $\gamma Q \to \gamma\gamma Q$. The corresponding processes for the QCD can be obtained by replacing the photons by gluons ($\gamma \leftrightarrow G$) in the final states. The key word in the above description is the word ''genuine'': By genuine *s*-channel part we mean the *s*-channel part obtained *after* the longitudinal terms of the polarization vectors involved have triggered the WIs of the various amplitudes. These WIs implement themselves in ways that do not respect the original *s*-*t* channel separation of the amplitude, as given by the Feynman graphs; instead, various *s*- and *t*-channel contributions are nontrivially mixed, in such ways as to finally result in fundamental cancellations. It turns out that all such contributions can again be pictorially represented by means of unphysical elementary vertices, a fact which facilitates significantly their identification.

In this section we will set up the formalism, adopted to the fermion self-energy, and discuss in detail the one-loop case; the two-loop generalization will be presented in Sec. IV.

A. QED

The optical theorem for the case of forward scattering assumes the form

$$\mathrm{Im}\langle a|T|a\rangle = \tfrac{1}{2}\sum_i (2\pi)^4 \delta^{(4)}(p_a - p_i) \times \langle i|T|a\rangle^* \langle i|T|a\rangle, \tag{3.1}$$

where the sum Σ_i should be understood to be over the entire phase space of all allowed on-shell intermediate states *i*. After expanding the T matrix in powers of g, i.e., $T = \Sigma_{n=2} T^{[n]}$, we have that

$$\mathrm{Im}\langle a|T^{[n]}|a\rangle = \tfrac{1}{2}\sum_i (2\pi)^4 \delta^{(4)}(p_a - p_i) \times \sum_k \langle i|T^{[k]}|a\rangle^* \langle i|T^{[n-k]}|a\rangle. \tag{3.2}$$

In the particular case of QED, if in the initial states we have a γQ i.e., $|a\rangle = |\gamma Q\rangle$, we have for the first nontrivial order, $n=4$, in the T

$$\mathrm{Im}\langle \gamma Q|T^{[4]}|\gamma Q\rangle = \tfrac{1}{2}\int (dPS)\langle \gamma Q|T^{[2]}|\gamma Q\rangle^* \times \langle \gamma Q|T^{[2]}|\gamma Q\rangle, \tag{3.3}$$

where (dPS) denotes the (two-body) phase-space integration. Next we introduce the short-hand notation

$$\mathcal{A}^{[n]} \equiv \mathrm{Im}\langle \gamma Q|T^{[n]}|\gamma Q\rangle, \qquad \mathcal{T}^{[k]} \equiv \langle \gamma Q|T^{[k]}|\gamma Q\rangle. \tag{3.4}$$

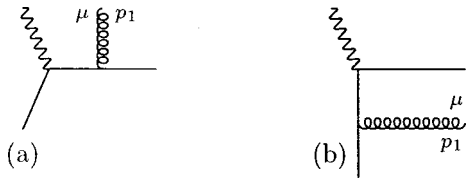

FIG. 4. The tree level one-particle phase space appearing in the one-loop QED absorptive PT construction. Diagram (a) defines the *s*-channel amplitude $\mathcal{T}_s^{[2]}$, while diagram (b) defines the *t*-channel amplitude $\mathcal{T}_t^{[2]}$.

To avoid notational clutter we will suppress the Lorentz index corresponding to the external photon. Using the above notation, and suppressing the phase-space integrations, we have

$$\mathcal{A}^{[4]} = \tfrac{1}{2}\mathcal{T}_\mu^{[2]} P^{\mu\mu'}(p_1)\mathcal{T}_{\mu'}^{[2]*}, \tag{3.5}$$

where $P_{\mu\nu}$ is the polarization tensor for photons or gluons,

$$P_{\mu\nu}(p,n,\eta) = -g_{\mu\nu} + \frac{n_\mu p_\nu + n_\nu p_\mu}{n\cdot p} - \eta\frac{p_\mu p_\nu}{(n\cdot p)^2}, \tag{3.6}$$

with n_μ being an arbitrary four-vector, and η a gauge parameter.

The amplitude $\mathcal{T}_\mu^{[2]}$ consists of *s*- channel and *t*-channel contributions, i.e.,

$$\mathcal{T}_\mu^{[2]} = \mathcal{T}_{s\mu}^{[2]} + \mathcal{T}_{t\mu}^{[2]} \tag{3.7}$$

(see Fig. 4). From the gauge symmetry we know that

$$p_1^\mu \mathcal{T}_\mu = 0, \tag{3.8}$$

to all orders. Clearly, by virtue of Eq. (3.8) all reference to the unphysical quantities n_μ and η disappears. We emphasize, however, that the action of the momentum p_1^μ does not respect the $s-t$ separation given by the initial set of Feynman diagrams. Instead, the action of p_1^μ gives rise to cancellations between the two sets. In particular we have that

$$p_1^\mu \mathcal{T}_{s\mu}^{[2]} = \mathcal{R}, \qquad p_1^\mu \mathcal{T}_{t\mu}^{[2]} = -\mathcal{R}$$

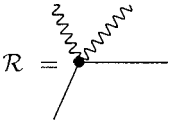

Notice that the term $\mathcal{R}$ contains always an unphysical vertex.

Therefore,

$$\mathcal{A}^{[4]} = \frac{1}{2}\mathcal{T}^{[2]} \otimes \mathcal{T}^{[2]*} = \frac{1}{2}(\mathcal{T}_s^{[2]} + \mathcal{T}_t^{[2]}) \otimes (\mathcal{T}_s^{[2]*} + \mathcal{T}_t^{[2]*}) = \mathcal{A}_{ss}^{[4]} + \mathcal{A}_{st}^{[4]} + \mathcal{A}_{tt}^{[4]}, \tag{3.9}$$

with

$$\mathcal{A}_{ss}^{[4]}=\tfrac{1}{2}\mathcal{T}_s^{[2]}\otimes\mathcal{T}_s^{[2]*},$$

$$\mathcal{A}_{st}^{[4]}=\tfrac{1}{2}(\mathcal{T}_s^{[2]}\otimes\mathcal{T}_t^{[2]*}+\mathcal{T}_t^{[2]}\otimes\mathcal{T}_s^{[2]*}), \qquad (3.10)$$

$$\mathcal{A}_{tt}^{[4]}=\tfrac{1}{2}\mathcal{T}_t^{[2]}\otimes\mathcal{T}_t^{[2]*}.$$

Next we will focus on $\mathcal{A}_{ss}^{[4]}$, which is the genuine *s*-channel part, i.e., the *s*-channel contribution after the longitudinal parts of $P^{\mu\mu'}(p_1)$ have been eliminated. We will cast $\mathcal{A}_{ss}^{[4]}$ in the form

$$\mathcal{A}_{ss}^{[4]}=(e\gamma_\alpha)S_0(p)A_{ss}^{[2]}(p)S_0(p)(e\gamma^\alpha), \qquad (3.11)$$

and then identify

$$\mathrm{Im}\hat{\Sigma}^{(1)}(p)=A_{ss}^{[2]}(p), \qquad (3.12)$$

where $\hat{\Sigma}^{(1)}(p)$ is the one-loop fermion self-energy under construction.

At this point it is straightforward to verify that

$$A_{ss}^{[2]}(p)=\mathcal{C}_2\{\hat{\Sigma}^{(1)}(p)\}=\mathcal{C}_2\{\Sigma_F^{(1)}(p)\}, \qquad (3.13)$$

where $\mathcal{C}_n\{\cdots\}$ is the operator which carries out the the *n*-particle Cutkosky cuts to the quantity appearing inside the curly brackets. In this case the two-particle cut involves a (massless) γ and a Q of mass m. The real part of $\hat{\Sigma}^{(1)}(p)$ can be obtained directly from $A_{ss}^{[2]}(p)$ by means of a (twice-subtracted) dispersion relation. In particular,

$$\mathrm{Re}\hat{\Sigma}^{(1)}(p)=\int_{t_2}^{\infty}dt\,\frac{A_{ss}^{[2]}(t)}{t-p^2}, \qquad (3.14)$$

where $t_2=m^2$ is the two-body threshold. After subtracting twice ''on-shell'' one obtains the corresponding renormalized quantity

$$\mathrm{Re}\hat{\Sigma}_R^{(1)}(p)=(p^2-m^2)^2\int_{t_2}^{\infty}dt\,\frac{A_{ss}^{[2]}(t)}{(t-p^2)(t-m^2)^2}. \qquad (3.15)$$

B. QCD

The one-loop QCD case can be directly derived from the QED analysis presented above. In particular, when applying the optical theorem one must consider a quark (Q) and a gluon (G) as an intermediate state, i.e.,

$$\mathrm{Im}\langle\gamma Q|T^{[4]}|\gamma Q\rangle=\tfrac{1}{2}\int(dPS)\times\langle GQ|T^{[2]}|\gamma Q\rangle^*\langle GQ|T^{[2]}|\gamma Q\rangle, \qquad (3.16)$$

and define the corresponding quantities (we suppress color)

$$\mathcal{A}^{[n]}\equiv\mathrm{Im}\langle\gamma Q|T^{[n]}|\gamma Q\rangle,$$
$$\mathcal{T}^{[k]}\equiv\langle GQ|T^{[k]}|\gamma Q\rangle. \qquad (3.17)$$

From this point on the analysis is exactly analogous to that presented for QED. The fact that the QED and QCD constructions coincide is special to the one-loop case and, as we will see in the next section, is not true in higher orders.

IV. THE TWO-LOOP ABSORPTIVE CONSTRUCTION

As mentioned at the beginning of the preceding section, in the two-loop case we have two distinct types of contributions: (i) those that are the one-loop corrections to the two-to-two particle process $\gamma Q\to\gamma Q$ ($\gamma Q\to GQ$ in the case of QCD), whose tree-level analysis was considered in the previous section; (ii) those that come from tree-level two-to-three particle processes.

There is one additional fact we will use in the analysis below: The one-loop contributions to $\gamma Q\to\gamma Q$ ($\gamma Q\to GQ$ in the case of QCD) considered in (i) can be effectively brought in the Feynman gauge, starting from any other gauge, using a procedure exactly analogous to that used in Sec. I. In particular, using nothing but elementary WIs, the reader should be able to see how all longitudinal contributions inside the Feynman diagrams of Fig. 5 are equivalent to unphysical vertices, which cancel algebraically.

Before we can proceed with the details of the two-loop absorptive construction, some additional comments are in order. In the previous section we have distinguished between the tree-level *s*-channel and *t*-channel contributions, shown in Fig. 4, using the obvious criterion of whether a diagram depends on the Mandelstam variable s [Fig. 4(a)] or t [Fig. 4(b)]. Notice, however, that in addition to the t variable, the *t-channel* fermion propagator in Fig. 4(b) depends explicitly on the mass of the incoming (test) fermion. A similar distinction between *s*-channel and *t*-channel contributions needs to be established in this section; however, additional care is needed when classifying the various diagrams. Clearly, diagrams that are one-loop corrections to the tree-level *t*-channel graph of Fig. 4(b), such as those shown in Figs. 5(e), 5(f), 5(g), 5(h), 5(m), 5(n), 5(p), and 5(q), will be characterized as *t*-channel graphs. In addition, those graphs that arise as one-loop vertex or wave-function corrections to the *incoming* particles of Fig. 4(a), such as Figs. 5(i) and 5(o), will also be classified as *t*-channel graphs. Finally, graphs as those shown in Figs. 5(a)–5(c), which are one-loop corrections to either the *s*-dependent off-shell propagator or vertex and wave-function corrections to the *outgoing* particles of the tree-level *s*-channel of Fig. 4(a), will be characterized as *s*-channel graphs. At first sight the characterization of the graphs in Figs. 5(i) and 5(o) as *t*-channel graphs may seem unusual, since there is no explicit t dependence in them; indeed, both graphs depend on s, but, in addition, on the masses of the incoming particles. Thus, in general, if such graphs were to be considered as parts of the two-loop self-energy which is being constructed absorptively, they would introduce in it an explicit process dependence. This would clearly be a drawback, since the off-shell gauge-invariant

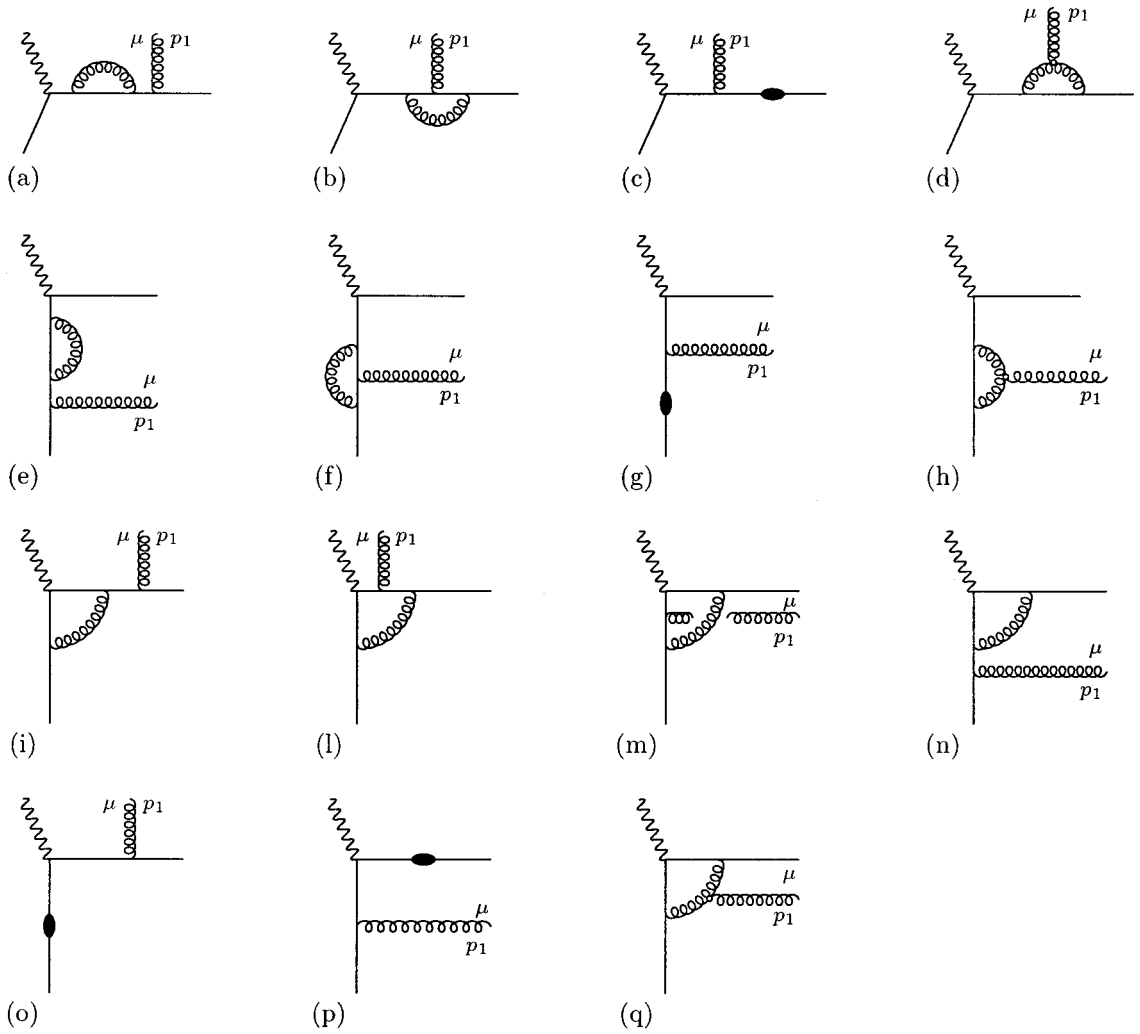

FIG. 5. The one-loop two-particle phase space appearing in the two-loop QCD absorptive PT construction. Diagrams (a),...,(d) define the *s*-channel amplitude $\mathcal{T}^{[2]}_{\mathrm{as}}$, while all the others define the *t*-channel amplitude $\mathcal{T}^{[2]}_{\mathrm{at}}$.

fermion self-energies one wants to define should be universal, i.e., process independent. To appreciate this point, let us imagine that instead of the flavor-conserving processes we consider here (in which case the mass of the incoming on-shell fermion is the same as that of the off-shell one, and the external photons are massless), we were instead studying a process containing a flavor-nonconserving interaction, such as $W^+b\to t\gamma$, or $W^+b\to tZ$ attempting to define absorptively the part of the off-shell top-quark (t) self-energy that contains a t and a γ or a t and a Z. In that case graphs such as those in Figs. 5(i) and 5(o), together with the W wave-function graphs (not shown), would introduce into the $t\gamma$ and tZ ''widths'' an unphysical dependence on m_b and M_W. Thus, according to this definition, the *s*-channel graphs are those graphs which do not contain information about the kinematical details of the incoming test particles.

A. QED

There are three different thresholds, to be denoted by $\mathfrak{a}\equiv\gamma Q$, $\mathfrak{b}\equiv\gamma\gamma Q$, and $\mathfrak{c}\equiv Q\bar{Q}Q$. Thus,

$$\begin{aligned}
&\mathrm{Im}\langle q\bar{q}|T^{[6]}|q\bar{q}\rangle\\
&\quad=\tfrac{1}{2}\int(dPS)_{\mathfrak{a}}2\,\mathrm{Re}[\langle\gamma Q|T^{[4]}|\gamma Q\rangle^*\langle\gamma Q|T^{[2]}|\gamma Q\rangle]\\
&\quad+\tfrac{1}{2}\int(dPS)_{\mathfrak{b}}\langle\gamma\gamma Q|T^{[3]}|\gamma Q\rangle^*\langle\gamma\gamma Q|T^{[3]}|\gamma Q\rangle\\
&\quad+\tfrac{1}{2}\int(dPS)_{\mathfrak{c}}\langle Q\bar{Q}Q|T^{[3]}|\gamma Q\rangle^*\langle Q\bar{Q}Q|T^{[3]}|\gamma Q\rangle.
\end{aligned}\tag{4.1}$$

Then we have, suppressing the phase-space integrations, and using the previously introduced notation

$$\begin{aligned}
\mathcal{A}^{[6]}&=\mathrm{Re}(\mathcal{T}^{[4]}_{\mathfrak{a}\mu}P^{\mu\mu'}(p_1)\mathcal{T}^{[2]*}_{\mathfrak{a}\mu'})\\
&\quad+\tfrac{1}{2}\mathcal{T}^{[3]}_{\mathfrak{b}\mu\nu}P^{\mu\mu'}(p_1)P^{\nu\nu'}(p_2)\mathcal{T}^{[3]*}_{\mathfrak{b}\mu'\nu'}\\
&\quad+\tfrac{1}{2}\mathcal{T}^{[3]}_{\mathfrak{c}}\mathcal{T}^{[3]*}_{\mathfrak{c}}\\
&\equiv\mathcal{A}^{[6]}_{\mathfrak{a}}+\mathcal{A}^{[6]}_{\mathfrak{b}}+\mathcal{A}^{[6]}_{\mathfrak{c}}.
\end{aligned}\tag{4.2}$$

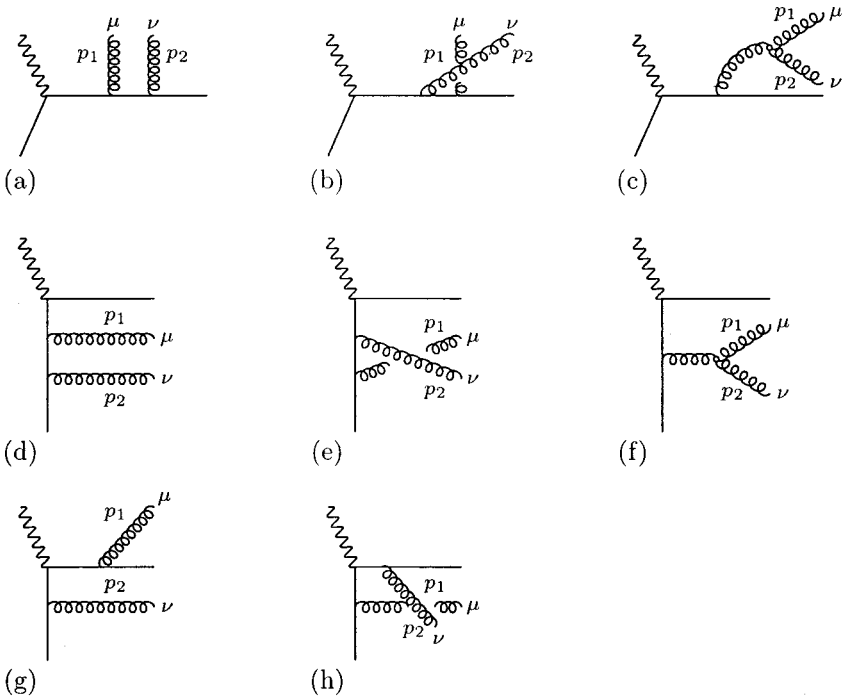

FIG. 6. The tree-level three-particle phase space appearing in the two-loop QCD absorptive PT construction. Diagrams (a),...,(c) define the *s*-channel amplitude $\mathcal{T}^{[3]}_{\mathfrak{b}s}$, while all the others define the *t*-channel one $\mathcal{T}^{[3]}_{\mathfrak{b}t}$.

From the gauge symmetry we know that

$$p_1^\mu \mathcal{T}_{\mathfrak{b}\mu\nu}=0,$$
$$p_2^\nu \mathcal{T}_{\mathfrak{b}\mu\nu}=0, \tag{4.3}$$

to all orders. Again, the same situation explained in the one-loop case is true now, namely the fact that the WI mixes contributions between the *s* and *t* channels, which all contain unphysical vertices. In particular, at order e^6,

$$p_1^\mu (\mathcal{T}^{[3]}_{\mathfrak{b}s})^\nu_\mu = \mathcal{R}^{[3]\,\nu}_{\mathfrak{b}}$$
$$p_1^\mu (\mathcal{T}^{[3]}_{\mathfrak{b}t})^\nu_\mu = -\mathcal{R}^{[3]\,\nu}_{\mathfrak{b}} \qquad \mathcal{R}^{[3]\,\nu}_{\mathfrak{b}} =$$

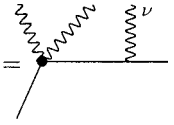

(4.4)

and an identical equation holds when contracting with $p_{2\nu}$. Notice that again the term $\mathcal{R}^{[3]\,\nu}$ contains an unphysical vertex.

Finally,

$$\mathcal{A}^{[6]}_{\mathfrak{i}}=\mathcal{A}^{[6]}_{\mathfrak{i}\,ss}+\mathcal{A}^{[6]}_{\mathfrak{i}\,st}+\mathcal{A}^{[6]}_{\mathfrak{i}\,tt}, \quad \mathfrak{i}=\mathfrak{a},\ \mathfrak{b},\ \mathfrak{c} \tag{4.5}$$

with

$$\mathcal{A}^{[6]}_{\mathfrak{a}\,ss}=\mathrm{Re}[\mathcal{T}^{[4]}_{\mathfrak{a}\,s}\otimes\mathcal{T}^{[2]*}_{\mathfrak{a}\,s}],$$
$$\mathcal{A}^{[6]}_{\mathfrak{a}\,st}=\mathrm{Re}[\mathcal{T}^{[4]}_{\mathfrak{a}\,s}\otimes\mathcal{T}^{[2]*}_{\mathfrak{a}\,t}+\mathcal{T}^{[4]}_{\mathfrak{a}\,t}\otimes\mathcal{T}^{[2]*}_{\mathfrak{a}\,s}], \tag{4.6}$$
$$\mathcal{A}^{[6]}_{\mathfrak{a}\,tt}=\mathrm{Re}[\mathcal{T}^{[4]}_{\mathfrak{a}\,t}\otimes\mathcal{T}^{[2]*}_{\mathfrak{a}\,t}],$$

and

$$\mathcal{A}^{[6]}_{\mathfrak{m}\,ss}=\tfrac{1}{2}\mathcal{T}^{[3]}_{\mathfrak{m}\,s}\otimes\mathcal{T}^{[3]*}_{\mathfrak{m}\,s},$$
$$\mathcal{A}^{[6]}_{\mathfrak{m}\,st}=\tfrac{1}{2}(\mathcal{T}^{[3]}_{\mathfrak{m}\,s}\otimes\mathcal{T}^{[3]*}_{\mathfrak{m}\,t}+\mathcal{T}^{[3]}_{\mathfrak{m}\,t}\otimes\mathcal{T}^{[3]*}_{\mathfrak{m}\,s}), \tag{4.7}$$
$$\mathcal{A}^{[6]}_{\mathfrak{m}\,tt}=\tfrac{1}{2}\mathcal{T}^{[3]}_{\mathfrak{m}\,t}\otimes\mathcal{T}^{[3]*}_{\mathfrak{m}\,t}, \quad \mathfrak{m}=\mathfrak{b},\ \mathfrak{c}.$$

Let us next consider the *ss* parts, $A^{[6]}_{\mathfrak{i}\,ss}(p)$. Unlike the one-loop case, where in Eq. (3.12) the entire *ss* part $A^{[2]}_{ss}(p)$ was identified with $\mathrm{Im}\,\hat{\Sigma}^{(1)}(p)$, now we must identify $A^{[6]}_{\mathfrak{i}\,ss}(p)$ with the imaginary parts of both the two-loop *one-particle irreducible* fermion self-energy $\hat{\Sigma}^{(2)}(p)$ and the one-particle reducible string of two $\hat{\Sigma}^{(1)}(p)$; of course the latter contributions are known from the one-loop construction of the previous section. Thus,

$$\mathrm{Im}\,\hat{\Sigma}^{(2)}(p)=A^{[6]}_{\mathfrak{i}\,ss}(p)-2\,\mathrm{Im}\,\hat{\Sigma}^{(1)}(p)\mathrm{Re}\,\hat{\Sigma}^{(1)}(p)$$
$$\equiv A^{[6]\ 1\mathrm{PI}}_{\mathfrak{i}\,ss}(p) \tag{4.8}$$

where the superscript ''1PI'' stands for ''one-particle irreducible.'' One can verify at this point that

$$A^{[6]\ 1\mathrm{PI}}_{\mathfrak{i}\,ss}(p)=\mathcal{C}_{\mathfrak{i}}\{\hat{\Sigma}^{(2)}(p)\}=\mathcal{C}_{\mathfrak{i}}\{\hat{\Sigma}^{(2)}_F(p)\}, \quad \mathfrak{i}=\mathfrak{a},\ \mathfrak{b},\ \mathfrak{c}. \tag{4.9}$$

Clearly, the two-particle cut involves a γ and a Q, whereas the three-particle cut involves two γ's and a Q, and three Q's, respectively. Of course, for massless photons the two cuts

coincide. The real part of $\hat{\Sigma}^{(2)}(p)$ can be obtained directly from the three quantities $A^{[6]}_{\mathfrak{i}\,ss}(p)$ by means of an appropriate dispersion relation. In particular,

$$\mathrm{Re}\,\hat{\Sigma}^{(2)}(p)=\sum_{\mathfrak{i}}\int_{t_{\mathfrak{i}}}^{\infty}dt\,\frac{A^{[6]\ 1\mathrm{PI}}_{\mathfrak{i}\,ss}(t)}{t-p^2}, \tag{4.10}$$

with $t_{\mathfrak{a}}=t_{\mathfrak{b}}=m^2$ and $t_{\mathfrak{c}}=9m^2$. Again, after subtracting twice "on shell," one obtains the corresponding renormalized quantity $\mathrm{Re}\,\hat{\Sigma}^{(2)}_R(p)$.

B. QCD

There are three different thresholds, to be denoted by $\mathfrak{a}\equiv GQ$, $\mathfrak{b}\equiv GGQ$, and $\mathfrak{c}\equiv Q\bar{Q}Q$. So, at order $e^2g_s^4$ we have

$$\begin{aligned}
&\mathrm{Im}\langle q\bar{q}|T^{[6]}|q\bar{q}\rangle\\
&\quad=\tfrac{1}{2}\int(dPS)_{\mathfrak{a}}2\,\mathrm{Re}[\langle GQ|T^{[4]}|\gamma Q\rangle^*\langle GQ|T^{[2]}|\gamma Q\rangle]\\
&\quad+\tfrac{1}{2}\int(dPS)_{\mathfrak{b}}\langle GGQ|T^{[3]}|\gamma Q\rangle^*\langle GGQ|T^{[3]}|\gamma Q\rangle\\
&\quad+\tfrac{1}{2}\int(dPS)_{\mathfrak{c}}\langle Q\bar{Q}Q|T^{[3]}|\gamma Q\rangle^*\langle Q\bar{Q}Q|T^{[3]}|\gamma Q\rangle.
\end{aligned} \tag{4.11}$$

We next turn to the tree-level WIs satisfied by the QCD amplitudes appearing above, when contacted by the momenta originating from the polarization tensor(s) of the final state gluon(s). To begin with, Eq. (4.2) holds exactly as in the QED case. It is worthwhile studying how this tree-level WI is realized at the diagrammatic level; a nontrivial interplay of terms containing unphysical vertices takes place, allowing contributions originating from different kinematic channels to cancel against each other. The diagrams contributing to the process $\gamma Q\to GQ$ at one loop are shown in Fig. 5. For brevity, we will illustrate the point by focusing only on the non-Abelian diagrams (d), (h), and (q) of Fig. 5. Using the elementary WI (2.18), we find the following equality:

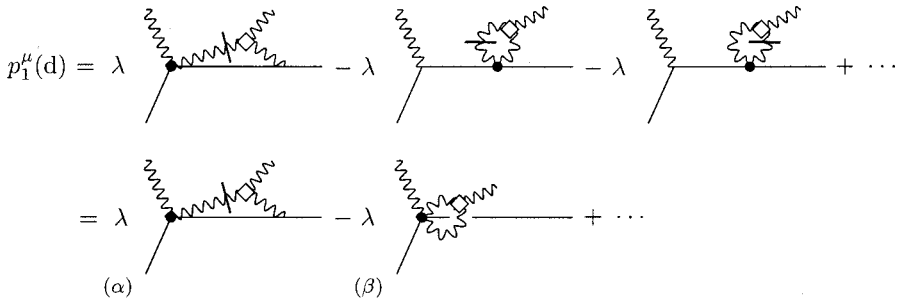

where the ellipses stand for diagrams that will cancel against contributions left over from the Abelian-like diagrams. Moreover, one has

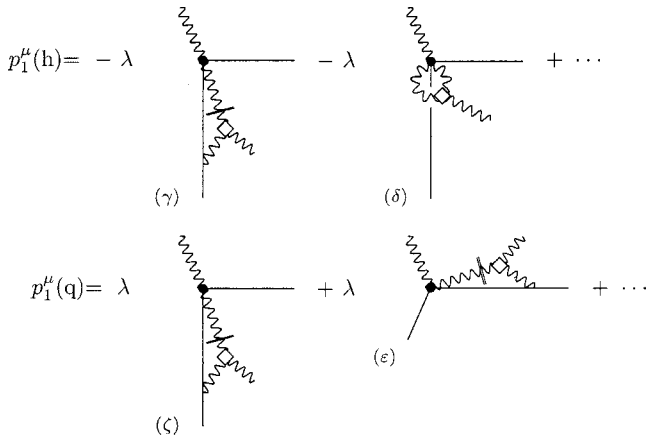

so that taking into account that diagrams (h) and (q) carry a (group-theoretical) relative minus sign with respect to diagram (d), we find the cancellations

$$(\alpha)+(\zeta)=0,\quad(\beta)+(\delta)=0,\quad(\gamma)+(\varepsilon)=0. \tag{4.12}$$

Thus, the analysis regarding the sector $\mathfrak{a}$ and $\mathfrak{c}$ is exactly analogous to that of QED. The only difference is related to the sector $\mathfrak{b}$, and originates from the fact that Eq. (4.3) and Eq. (4.4) are altered, due to the appearance of ghost-related contributions. In particular,

$$\begin{aligned}
p_1^\mu(\mathcal{T}^{[3]}_{\mathfrak{b}\,s})^\nu_\mu&=\mathcal{S}^{[3]}_{\mathfrak{b}\,s}p_2^\nu+\mathcal{R}^{[3]\ \nu}_{\mathfrak{b}},\\
p_1^\mu(\mathcal{T}^{[3]}_{\mathfrak{b}\,t})^\nu_\mu&=\mathcal{S}^{[3]}_{\mathfrak{b}\,t}p_2^\nu-\mathcal{R}^{[3]\ \nu}_{\mathfrak{b}},
\end{aligned} \tag{4.13}$$

and by Bose symmetry the same equation is valid when $p_1 \leftrightarrow p_2$, and $\mu \leftrightarrow \nu$. In addition, acting with p_2^ν on both sides of Eq. (4.13), and using the on-shell conditions $p_1^2 = p_2^2 = 0$ we have

$$p_1^\mu p_2^\nu \mathcal{T}^{[3]}_{\mathfrak{b}\,\mu\nu} = 0. \tag{4.14}$$

To see how this WI is enforced diagrammatically, we next turn to the set of diagrams contributing to the tree-level two-to-three process, listed in Fig. 6. Contracting with the external momenta k_1^μ, taking into account the different color structure of the diagrams, and recalling the elementary WI (1.7), we obtain

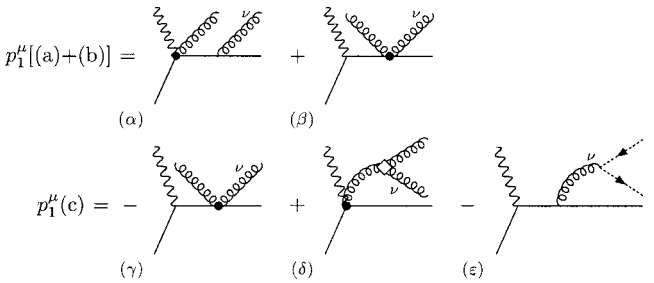

The cancellation between diagrams (β) and (γ) corresponds to the standard BRS-enforced s-t-channel cancellation [26] taking place in the tree-level amplitude $QQ \to GG$, which now appears embedded as a subprocess in the amplitude $\gamma Q \to GGQ$ that we consider here. As happens in the case of the $QQ \to GG$ example, the diagram (ε) gives rise to the correct ghost structure. Diagrams (α) and (δ), which contain external unphysical vertices, will cancel against similar contributions originating from the t-channel graphs. Specifically,

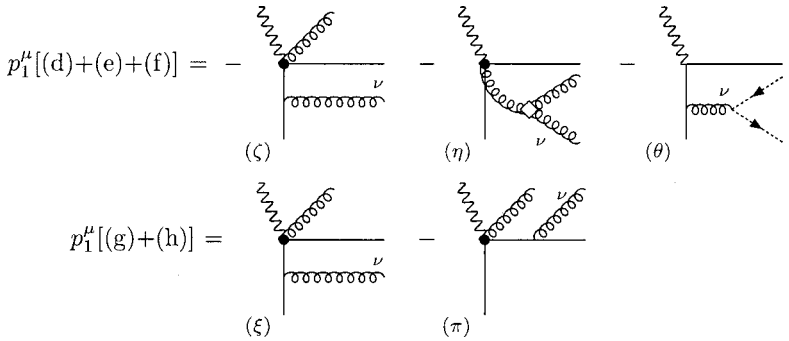

We can then identify the cancellations

$$(\alpha)+(\pi)=0, \quad (\delta)+(\eta)=0, \quad (\zeta)+(\xi)=0, \tag{4.15}$$

so that we are left only with the correct ghost structures, i.e., diagrams (ε) and (θ).

Thus, whereas Eq. (4.6) and the part of Eq. (4.7) with $\mathfrak{i} = \mathfrak{c}$ remain unchanged, the part of Eq. (4.7) with $\mathfrak{i} = \mathfrak{b}$ gets modified as follows:

$$\begin{aligned}
\mathcal{A}^{[6]}_{\mathfrak{b}\,ss} &= \tfrac{1}{2}(\mathcal{T}^{[3]}_{\mathfrak{b}\,s} \otimes \mathcal{T}^{[3]}_{\mathfrak{b}\,s}{}^{*} - 2\mathcal{S}^{[3]}_{\mathfrak{b}\,s} \otimes \mathcal{S}^{[3]}_{\mathfrak{b}\,s}{}^{*}), \\
\mathcal{A}^{[6]}_{\mathfrak{b}\,st} &= \tfrac{1}{2}[(\mathcal{T}^{[3]}_{\mathfrak{b}\,s} \otimes \mathcal{T}^{[3]}_{\mathfrak{m}\,t}{}^{*} - 2\mathcal{S}^{[3]}_{\mathfrak{b}\,s} \otimes \mathcal{S}^{[3]}_{\mathfrak{b}\,t}{}^{*}) + (\mathcal{T}^{[3]}_{\mathfrak{b}\,t} \otimes \mathcal{T}^{[3]}_{\mathfrak{b}\,s}{}^{*} \\
&\quad - 2\mathcal{S}^{[3]}_{\mathfrak{b}\,t} \otimes \mathcal{S}^{[3]}_{\mathfrak{b}\,s}{}^{*})], \\
\mathcal{A}^{[6]}_{\mathfrak{b}\,tt} &= \tfrac{1}{2}(\mathcal{T}^{[3]}_{\mathfrak{b}\,t} \otimes \mathcal{T}^{[3]}_{\mathfrak{b}\,t}{}^{*} - 2\mathcal{S}^{[3]}_{\mathfrak{b}\,t} \otimes \mathcal{S}^{[3]}_{\mathfrak{b}\,t}{}^{*}).
\end{aligned} \tag{4.16}$$

Beyond this point it is easy to see that the analysis following Eq. (4.7) of the QED case applies unchanged to the QCD case as well.

V. DISCUSSION AND CONCLUSIONS

In this paper we have shown *explicitly* that the off-shell two-loop fermion self-energy constructed by means of the PT *coincides* with the conventional fermion self-energy calculated in the covariant (renormalizable) Feynman gauge. This has been demonstrated by systematically tracking down the action of all terms originating from the longitudinal parts of the tree-level gauge boson propagators (photons or gluons) appearing inside the Feynman diagrams contributing to manifestly gauge-invariant amplitudes. It turns out that all such terms give rise to unphysical vertices, which cancel diagrammatically in the entire physical amplitude, without affecting the kinematical structure of the various subamplitudes (propagators, vertices, boxes). We have followed two different but physically equivalent approaches. First we have shown the cancellations at the level of the full two-loop amplitude. Then we have shown the cancellations for the two- and three-body cross sections which appear on the right-hand side of the optical theorem.

It is worth commenting on the relation of the results established here and those appearing in [18]. That work was an early attempt to define what the pinch technique should be

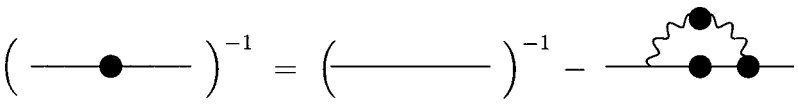

FIG. 7. The SD equation for the electron propagator S.

beyond one loop. At the time it was written the central issue had been how to deal with the internal three-gluon vertices appearing inside Feynman diagrams, i.e., three-gluon vertices all three legs of which are associated with gauge field propagating inside the loop. In particular, one needed to establish a well-defined criterion which would allow one to unambiguously decide whether and how the internal vertices should be split into pinching and nonpinching parts. What was proposed in [18] was to split the internal vertices following as a guiding principle some type of skeleton expansion of the quark two-loop self-energy. In particular, the starting point for the construction has been the general diagrammatic representation of the two-loop quark self-energy in terms of renormalized one-loop two-point and three-point functions and tree-level Bethe-Salpeter-type quark-gluon scattering kernel insertions in the one-loop quark self-energy. According to this construction, even if one were to start out in the Feynman gauge, pinching momenta stemming from the internal three-gluon vertex in the diagram of Fig. 3(t) [or Fig. 3(u)] would give rise to pinch contributions which should be removed from the effective PT propagator under construction. Thus, the final answer differs from that of the Feynman gauge; in fact, it does not coincide with any of the known gauges. However, this procedure was in contradiction with the already existing absorptive PT constructions [14,27], according to which the imaginary parts of the PT Green's functions are related by means of the optical theorem to precisely identifiable parts of physical cross sections. These latter parts are constructed by using again the PT rearrangement, but this time not at the level of amplitudes (S-matrix elements) but at the level of cross sections. This fundamental PT property relating real and imaginary parts is a nontrivial realization of the optical theorem at the level of individual Green's functions. As has been explained in detail in [16], any attempt to rearrange the internal vertices leads to a violation of the aforementioned property; therefore internal three-gluon vertices should remain unchanged, and only external ones need be modified. Therefore, in the case of the fermion propagator the only pinching momenta originate from the longitudinal parts of the internal gluon propagators.

If one accepts that the cancellation mechanism presented here persists to all orders, then so does the main result of this paper, namely that the PT fermion self-energy coincides with that in the Feynman gauge. This is so because, as already mentioned earlier, in the case of the fermion self-energy all three-boson vertices are ''internal,'' i.e., there are no further pinching contributions stemming from the usual PT rearrangement of three-boson vertices. Should that be the case, it would be interesting to study the form of the SD this self-energy satisfies. For example, the SD equation for the electron propagator S will be given by (see Fig. 7)

$$S^{-1}(p)=S_0^{-1}(p)-e^2 \times\int\frac{d^dk}{(2\pi)^d}\,\gamma_\mu S(p+k)\Gamma_\nu(p,k)\Delta^{\mu\nu}(k), \tag{5.1}$$

where $\Gamma_\nu(p,k)$ is the full photon-electron-electron vertex, and the full photon propagator $\Delta_{\mu\nu}$ now assumes the form

$$\Delta_{\mu\nu}(q)=(g_{\mu\nu}-q_\mu q_\nu/q^2)[q^2-\Pi(q)]^{-1}+q_\mu q_\nu/q^4 \tag{5.2}$$

where the scalar quantity $\Pi(q)$ is related to the full vacuum polarization $\Pi_{\mu\nu}$ by

$$\Pi_{\mu\nu}=(g_{\mu\nu}-q_\mu q_\nu/q^2)\Pi(q). \tag{5.3}$$

It will be interesting to study this form of the SD equation and its implication for fermion mass generation, particularly in the cases QED_3 and QED_4. Notice that the presence of $\Gamma_\nu(p,k)$ forces one to solve a system of coupled SD equations, or, alternatively, resort to a gauge-technique inspired Ansatz for $\Gamma_\nu(p,k)$ [28].

It is well known that one can construct a gauge-invariant operator out of a gauge-variant one by means of a path-order exponential containing the gauge field A [29]. In the case of the fermion propagator $S(x,y)=\langle 0|\psi(x)\bar{\psi}(y)|0\rangle$ the corresponding gauge-invariant propagator $S_{\rm PO}$ reads (''PO'' stands for ''path-ordered'')

$$S_{\rm PO}(x,y)=\langle 0|\psi(x)P\exp\left(i\int_x^y dz\cdot A(z)\right)\times\bar{\psi}(y)|0\rangle. \tag{5.4}$$

It would be interesting to explore possible connections between the path-ordered propagator and the PT propagator constructed in this paper, together with various other related formalisms, which have appeared in the literature [30,31].

Finally, it would be important to extend the methodology and results of this paper to the case of the electroweak sector of the standard model, especially given the phenomenological relevance of (resonant) top-quark production.

ACKNOWLEDGMENTS

The work of D.B. is supported by the Ministerio of Educación, Cultura y Deporte, Spain, under Grant No. DGICYT-PB97-1227, and the research of J.P. is supported by CICYT, Spain, under Grant No. AEN-99/0692.

[1] K. Johnson, M. Baker, and R. Willey, Phys. Rev. **136**, B1111 (1964); S. L. Adler and W. A. Bardeen, Phys. Rev. D **4**, 3045 (1971); **6**, 734(E) (1971); T. Maskawa and H. Nakajima, Prog. Theor. Phys. **52**, 1326 (1974); **54**, 860 (1975); V. A. Miransky, Phys. Lett. **91B**, 421 (1980); P. I. Fomin, V. P. Gusynin, V. A. Miransky, and Y. A. Sitenko, Riv. Nuovo Cimento **6N5**, 1 (1983).

[2] K. D. Lane, Phys. Rev. D **10**, 2605 (1974); K. Higashijima, *ibid.* **29**, 1228 (1984); H. Pagels, *ibid.* **19**, 3080 (1979); D. Atkinson and P. W. Johnson, *ibid.* **37**, 2290 (1988); C. D. Roberts and B. H. McKellar, *ibid.* **41**, 672 (1990).

[3] N. Dorey and N. E. Mavromatos, Phys. Lett. B **250**, 107 (1990); N. Dorey and N. E. Mavromatos, Nucl. Phys. **B386**, 614 (1992); N. E. Mavromatos, Nucl. Phys. B (Proc. Suppl.) **33C**, 145 (1993); N. E. Mavromatos and J. Papavassiliou, Phys. Rev. D **60**, 125008 (1999).

[4] For example, T. Appelquist, D. Carrier, L. C. Wijewardhana, and W. Zheng, Phys. Rev. Lett. **60**, 1114 (1988); T. Appelquist, K. D. Lane, and U. Mahanta, *ibid.* **61**, 1553 (1988).

[5] C. N. Leung, S. T. Love, and W. A. Bardeen, Nucl. Phys. **B323**, 493 (1989).

[6] D. K. Hong, V. A. Miransky, I. A. Shovkovy, and L. C. Wijewardhana, Phys. Rev. D **61**, 056001 (2000); **62**, 059903(E) (2000).

[7] W. A. Bardeen, C. T. Hill, and M. Lindner, Phys. Rev. D **41**, 1647 (1990).

[8] J. M. Cornwall, R. Jackiw, and E. Tomboulis, Phys. Rev. D **10**, 2428 (1974).

[9] W. J. Marciano and H. Pagels, Phys. Rep. **36**, 137 (1978).

[10] D. Atkinson and P. W. Johnson, J. Math. Phys. **28**, 2488 (1987); D. Atkinson, P. W. Johnson and K. Stam, Phys. Rev. D **37**, 2996 (1988).

[11] A. Pilaftsis, Z. Phys. C **47**, 95 (1990).

[12] J. M. Cornwall, Phys. Rev. D **26**, 1453 (1982); J. M. Cornwall and J. Papavassiliou, *ibid.* **40**, 3474 (1989); J. Papavassiliou, Phys. Rev. D **41**, 3179 (1990).

[13] A. A. Slavnov, Teor. Mat. Fiz. **10** 153 (1972) [Theor. Math. Phys. **10**, 99 (1972)]; J. C. Taylor, Nucl. Phys. **B33**, 436 (1971).

[14] J. Papavassiliou and A. Pilaftsis, Phys. Rev. Lett. **75**, 3060 (1995); Phys. Rev. D **53**, 2128 (1996).

[15] A. Denner, G. Weiglein, and S. Dittmaier, Phys. Lett. B **333**, 420 (1994); S. Hashimoto, J. Kodaira, Y. Yasui, and K. Sasaki, Phys. Rev. D **50**, 7066 (1994).

[16] J. Papavassiliou, Phys. Rev. Lett. **84**, 2782 (2000); Phys. Rev. D **62**, 045006 (2000).

[17] J. Papavassiliou, Phys. Rev. D **51**, 856 (1995).

[18] N. J. Watson, Nucl. Phys. **B552**, 461 (1999).

[19] Y. Yamada, Phys. Rev. D **64**, 036008 (2001).

[20] Y. J. Feng and C. S. Lam, Phys. Rev. D **53**, 2115 (1996).

[21] Y. L. Dokshitzer, D. Diakonov, and S. I. Troian, Phys. Rep. **58**, 269 (1980); A. Andrasi and J. C. Taylor, Nucl. Phys. **B192**, 283 (1981); D. M. Capper and G. Leibbrandt, Phys. Rev. D **25**, 1002 (1982).

[22] G. Leibbrandt, Phys. Rev. D **29**, 1699 (1984); Rev. Mod. Phys. **59**, 1067 (1987); G. Leibbrandt and J. Williams, Nucl. Phys. **B440**, 573 (1995); **B566**, 373 (2000).

[23] C. Becchi, A. Rouet, and R. Stora, Ann. Phys. (N.Y.) **98**, 287 (1976).

[24] J. Papavassiliou and A. Pilaftsis, Phys. Rev. D **54**, 5315 (1996).

[25] N. K. Nielsen, Nucl. Phys. **B97**, 527 (1975).

[26] See, e.g., T.-P. Cheng and L.-F. Li, *Gauge Theory of Elementary Particle Physics* (Clarendon Press, Oxford, 1985), p. 277.

[27] J. Papavassiliou, E. de Rafael, and N. J. Watson, Nucl. Phys. **B503**, 79 (1997).

[28] A. Salam, Phys. Rev. **130**, 1287 (1963); R. Delbourgo and A. Salam, *ibid.* **135**, B1398 (1964); R. Delbourgo and P. West, J. Phys. A **10**, 1049 (1977); R. Delbourgo, Nuovo Cimento A **49**, 484 (1979); D. Atkinson, P. W. Johnson, and P. Maris, Phys. Rev. D **42**, 602 (1990).

[29] K. G. Wilson and J. B. Kogut, Phys. Rep. **12**, 75 (1974).

[30] S. Catani and E. D'Emilio, Fortschr. Phys. **41**, 261 (1993).

[31] E. Bagan, M. Lavelle, and D. McMullan, Phys. Rev. D **56**, 3732 (1997).